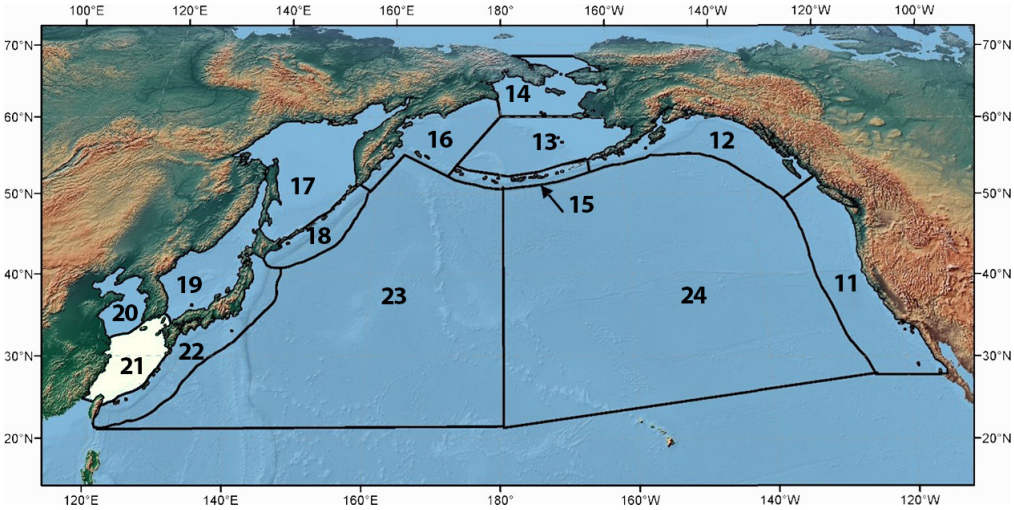

PICES

Regional Report for PICES Region: 21

PICES SPECIAL PUBLICATION 7

Marine Ecosystems of the North Pacific Ocean 2009–2016

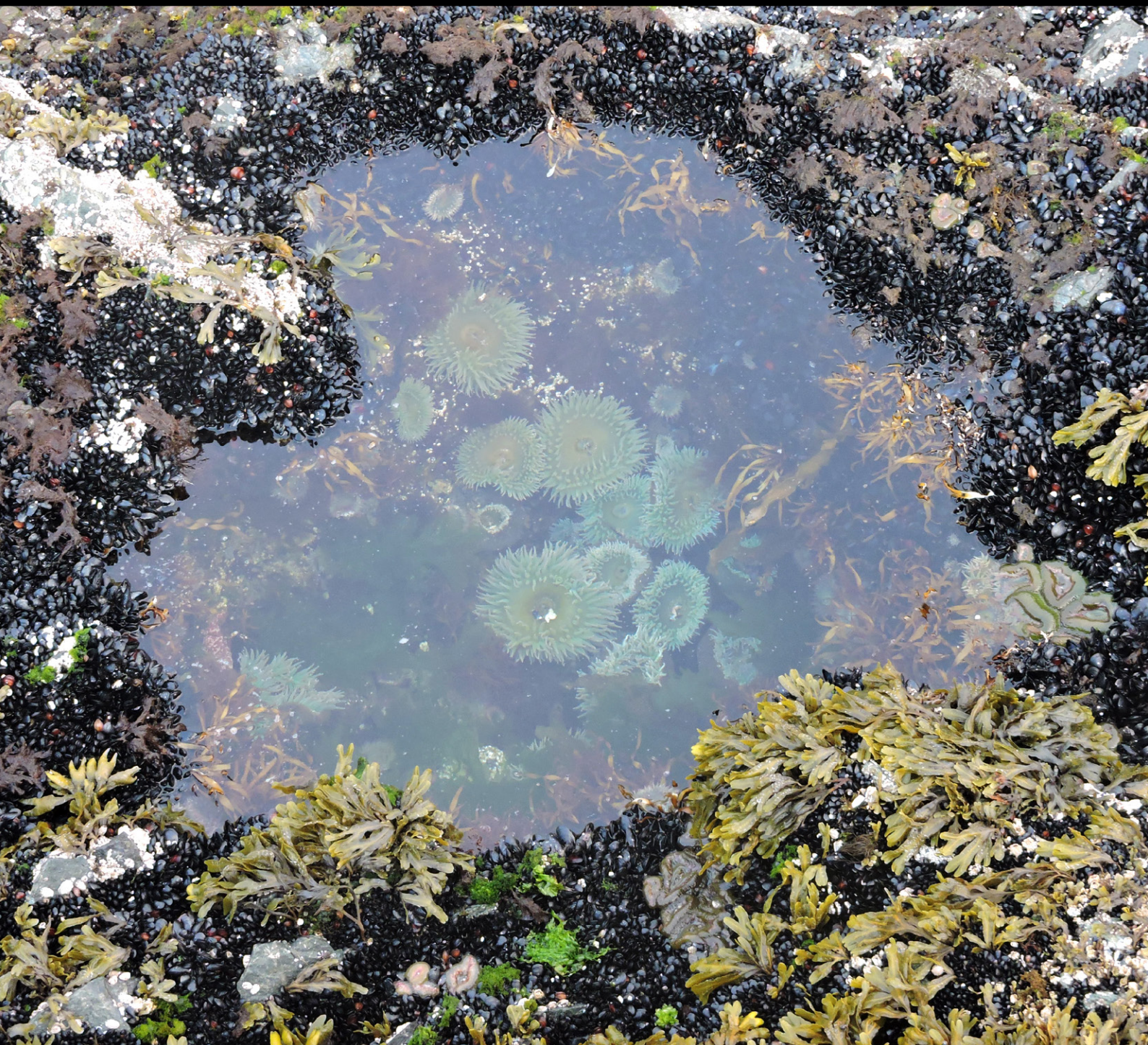

PICES North Pacific Ecosystem Status Report, Region 21 (East China Sea)

Yu Fei[1,2,3,4,5]

[1] Institute of Oceanology, Chinese Academ1y of Sciences, Qingdao, China
[2] University of Chinese Academy of Sciences, Beijing, China
[3] CAS Key Laboratory of Ocean Circulation and Waves, Chinese Academy of Sciences, Qingdao 266071, China
[4] Center for Ocean Mega-Science, Chinese Academy of Sciences, Qingdao 266071, China
[5] Marine Dynamic Process and Climate Function Laboratory, Pilot National Laboratory for Marine Science and Technology (Qingdao), Qingdao 266237, China

Contributors:

Xinyu Guo, Byoung-Ju Choi and Fangli Qiao, Dongfeng Xu SungHyun Nam, Hailun He, Takeshi Matsuno, Hao Wei, Jae Hak Lee, Chuanjie Wei, Sang-Wook Yeh, Guiling Zhang, Wang-Wang Ye, Sumei Liu, Yu Umezawa, Zhuoyi Zhu, Jing Zhang, Guebuem Kim, Wuchang Zhang, Chung Yeon Hwang, Hiroshi Koshikawa, Jae Hoon Noh, Yuan Zhao, Joji Ishizaka, Guangtao Zhang, Xinzheng Li, Yong Xu, Weiwei Xian and Cui Liang

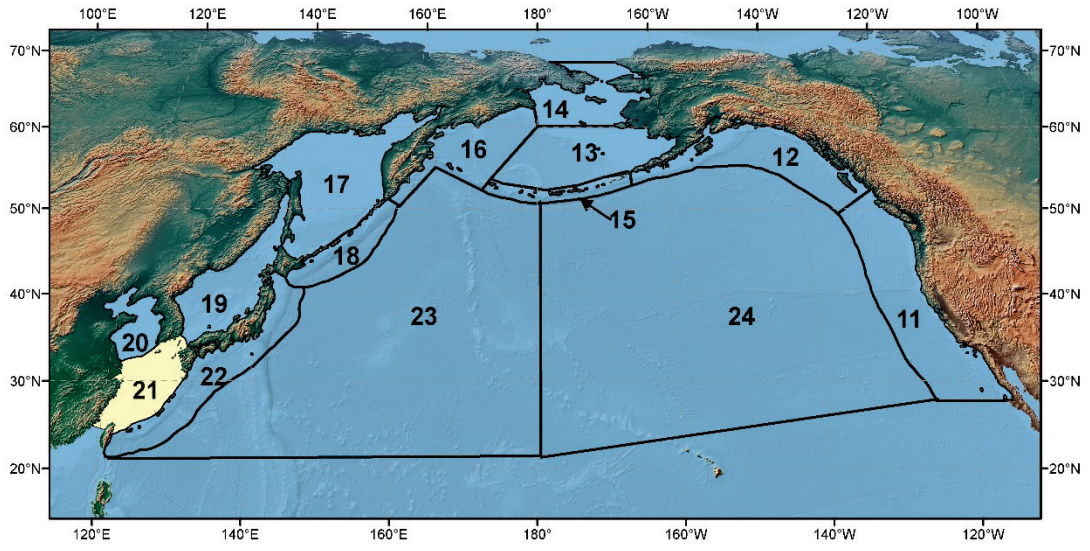

Figure R21-1. The PICES biogeographical regions and naming convention for the North Pacific Ocean with the area discussed in this report highlighted.

1. Highlights

- Under a Global Warming background, the East China Sea showed a warming trend. The area around the Changjiang estuary has the highest rate of rising temperature.
- Oxygen depletion has become more severe in recent decades, The biggest hypoxic zone is located in the region off the Changjiang Estuary in the adjacent East China Sea, with the largest regions covering an area of 15,400 km^2.
- More red tide events are happening in the East China Sea, and more attention is being paid to the ecosystem and phytoplankton in this area and their relationship to human activities and climate change.

2. Introduction

The East China Sea (ECS) is a marginal sea east of China. It is a part of the Pacific Ocean and covers an area of roughly 1,249,000 km^2. The ECS is bounded to the north by the Yellow Sea, to the east by the Japanese islands of Kyushu and Ryukyu, and to the west by the Asian continent. It is also connected to other marginal seas through the Korea (Tsushima) Strait to the northeast and through the Taiwan Strait to the southwest. The countries that border the ECS are Korea, Japan, and China.

The ECS has not only a shelf area but also a sharp slope and deep-water areas. Consequently, it has an average water depth of 370 m and a maximum of 2940 m. Two-thirds of the ECS is on the continental shelf and this part is separated into an inner shelf, middle shelf and outer shelf by 50-m, 100-m and 200-m isobaths. The isobaths over the continental shelf are basically parallel to the coastline. Outside the continental shelf is the Okinawa Trough with a depth of 600 to 2000 m.

The Changjiang (Yangtze) River, the largest river in Euro-Asian continent, drains more than 1.80×10^6 km^2, and is the third, fourth and fifth largest river in the world in terms of length, sediment yield and discharge, respectively. The Changjiang River estuary, at the junction of the Yellow Sea and the East China Sea, is the connected link between the Changjiang River and East China Sea. A large amount of freshwater and terrigenous materials is injected into the estuary annually, which sustains productive fishery grounds, the Zhoushan and Lüsi fisheries, in the adjacent seas (Tian et al., 1993; Chen et al., 2001), and provides a changeable environmental condition for estuarine organisms.

3. Physical Oceanography

The Kuroshio enters the ECS through the east coast of Taiwan and the southernmost one of the Ryukyu Islands chain. Under the constraint of the ECS continental slope, the main stream of the Kuroshio in the ECS runs stably along the 200-m isobath at a maximum velocity of 0.75–1.5 m s^{-1} (Nitanni, 1972). Passing through the Okinawa Trough, the Kuroshio hugs the shelf break of the ECS until it approaches the shoaling northern end of the trough, where it separates from the shelf and bends east–southeastward. After it turns eastward around 30°29′N, 129°E (Qiu and Imasato, 1990), the Kuroshio separates from the continental margin, and eventually flows into the Pacific Ocean through the Tokara Strait. The Kuroshio intrudes into the ECS from the subsurface water of the Kuroshio northeast of Taiwan, upwells northwestward gradually from 300 to 60 m, then turns to northeast in the region around 27.5°N, 122°E, and finally reaches 31°N off the mouth of the Changjiang River along approximately the 60-m isobath, forming bottom saline water off the coast of Zhejiang Province (Yang et al., 2011). The Kuroshio has been known to have two branch currents entering the continental shelf of the ECS: the Taiwan Warm Current in the southwestern ECS and the Tsushima Warm Current in the southeastern ECS (e.g., Guan and Mao, 1982). The two branches have a strong influence on water circulation and water mass distribution not only in the ECS, but also in the Yellow Sea (e.g., Kondo, 1985).

The Taiwan Warm Current (TWC) refers to the northward movement of warm water off the Min-Zhe coasts of China, and was first observed in the late 1950s (Guan and Chen, 1964). Originating from the Kuroshio, the TWC runs through the middle continental shelf and intrudes into the inner continental shelf outside the Changjiang mouth, influencing the coastal ecological, chemical and physical environments by transporting warm, saline and oligotrophic open ocean materials across the shelf into the ECS (e.g., Miao and Yu, 1991; Zhang, J. et al., 2007). The TWC originates from two parts of waters (see Figure R21-2). One is the Taiwan Strait Current (TSC) from Taiwan Strait (Su et al., 1994) and the other is the Kuroshio Branch Current to the northeast of Taiwan (KBCNT) (Kondo, 1985; Ichikawa and Beardsley, 2002; Yang et al., 2011; Lian et al., 2016). The high salinity lower TWC water is considered to be derived from the KBCNT, and the high temperature and less saline surface TWC water originates both from the TSC and the KBCNT (Weng and Wang, 1984). As proposed by Su and Pan [1987], the TWC bifurcates into two branches near 28°N within the middle continental shelf: the inshore branch (TWCIB; this is the traditional TWC) which flows northward along approximately the 50-m isobath off the Min-Zhe coasts and turns to the northeast off the mouth of the Changjiang River, and offshore branch (TWCOB) which first flows anticyclonically, then turns cyclonically and finally joins the western flank of the Kuroshio. However, there is no agreement on where the north end of the TWCIB is because of a lack of long-term currents observations.

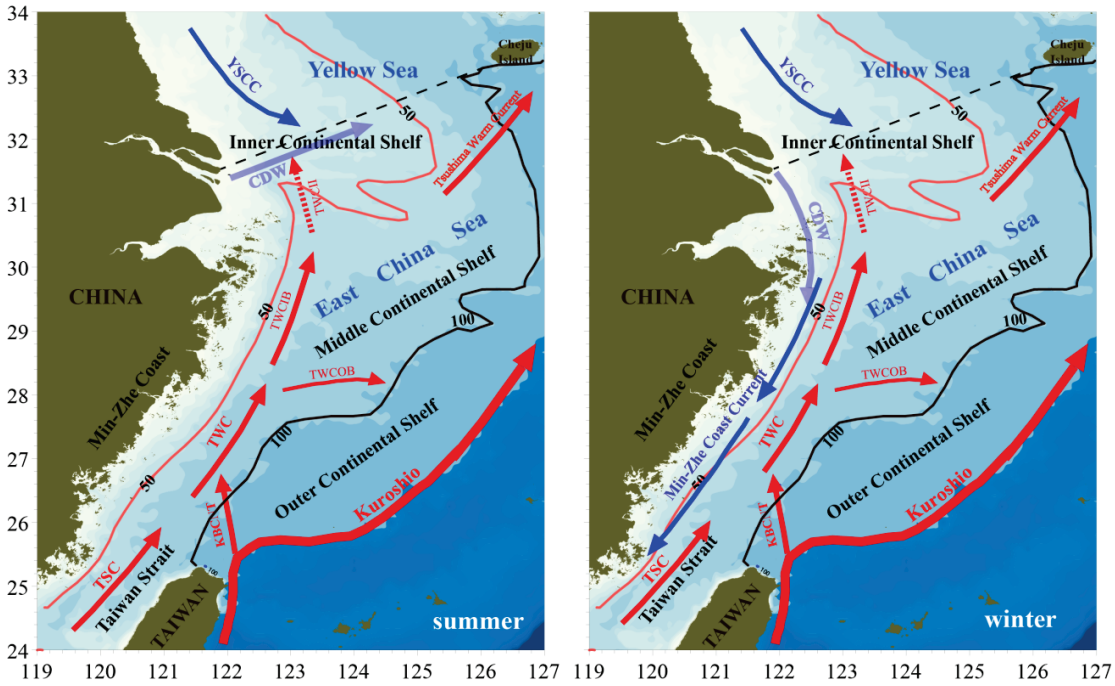

Figure R21-2. Schematic circulation patterns in the ECS. Left panel indicates the circulation in summer and right panel indicates the circulation in winter. TSC = Taiwan Strait Current, TWC = Taiwan Warm Current, TWCIB/TWCOB = TWC inshore branch/offshore branch, CDW = Changjiang Diluted Water.

The Tsushima Warm Current carries volume, heat, and salt from ECS to the east and has a large impact on the surface circulation in Region19. The scientific questions for the Tsushima Warm Current in the ECS are the origin of the Tsushima Warm Current and its volume. In general, there are two points of view on the origin of the Tsushima Warm Current. The first one is that it is considered as a northward branch of the Kuroshio when it separates southwest of Kyushu and that the Yellow Sea Warm Current (YSWC), separated from the Tsushima Warm Current southeast of Cheju Island, flows into the eastern Yellow Sea (Nitani, 1972). This point is supported by trajectories of satellite-tracked drifters (Lie and Cho, 1994). The second point is that the TWC originates mainly from the Taiwan Strait (Beardsley et al., 1985). This was supported by current meter data over the continental shelf of the ECS (Fang et al., 1991). The volume transport of the Tsushima Warm Current is estimated from ferryboat acoustic Doppler current profiler (ADCP) data (Takikawa et al., 2005) and numerical models (Guo et al., 2006). The debates over the origin and volume of the Tsushima Warm Current are induced by lack of long-term direct current measurements.

The coastal currents in the ECS are complicated. Along the southern coast of the ECS, the northward flow through the Taiwan Strait is called the Taiwan Strait Warm Current (TSWC). TSWC is reported flow northward along the Fujian-Zhejiang coast all year round, downwind in summer and upwind in winter (Su and Wang, 1987; Guan

and Fang, 2006). As an extension of the South China Sea Warm Current (SCSWC), the TSWC brings high temperature and salinity South China Sea water into the ECS (Hu and Liu, 1992). Paralleling the TSWC on the coastal side, the Min-Zhe Coastal Current (MZCC) exists in winter, induced by the winter monsoon, while there is no evidence of the existence of the MZCC in summer during the south summer monsoon. Along the southern coast in the ECS, the Yellow Sea Coastal Current (YSCC) moves southward in winter, but there is a conflict in the direction (Liu and Hu, 2009) of the YSCC in summer because lack of direct current measurements. The YSCC plays an important role in the evolution of the ECS water masses. Specifically it causes the intensification of the MZCC and the YSWC water, and blocks the northeastward dispersion of the TWC water (Li et al., 2006).

Freshwater output from the Changjiang River forms a large-scale plume, which plays a key role in physical processes in the adjacent ECS. This water flux, known as Changjiang diluted water (CDW), is a prominent hydrographic feature in the ECS. In summer, the CDW extends northeastward and forms a surface plume, while in winter it flows south in a narrow band along the eastern Chinese coast. The Changjiang River carries an enormous volume of fresh water, sediments, and nutrients to the ECS, which significantly influences the water properties, circulation structure, sediment deposition, and ecosystems of the adjacent seas (Beardsley et al., 1985; Zhu and Shen, 1997). The influence of the Changjiang River on the water masses in the ECS is through the spreading of riverine plumes. The spreading of the plumes is strongly influenced by river discharge (Le, 1984), the East Asia monsoon (Zhu and Shen, 1997; Chang and Isobe, 2003), tidal mixing (Wu et al., 2011), coastal currents (Zhu et al., 1998), and continental-shelf circulation. Mao et al. (1963) first found that the CDW turns to the northeast in summer, using salinity data, but not to the south as would be expected, driven by the Coriolis force. The southerly summer monsoon is the dominant factor in the northeastward extension of the plume (Zhu and Shen, 1997; Chang and Isobe, 2003). In summer, the far-field diluted Changjiang water joins the northeastward shelf–current system and flows out of the ECS through the Tsushima Strait where the year-round freshwater outflow is estimated to be at least 70% of the total Changjiang river discharge (Isobe et al., 2002; Chang and Isobe, 2003). In winter the CDW riverine plume flows south in a narrow band confined to the coast (e.g., Mao et al., 1963; Beardsley et al., 1985; Zhu and Shen, 1997).

Previous studies on the ECS focus on typical seasons such as summer and winter. Because current observations are limited, mostly previous studies are used to classify water masses according to the characteristic temperature and salinity, using different analysis methods of water masses such as similar coefficients (Weng and Wang, 1984) and clustering method (Su and Weng, 1994; Qi et al., 2014). However, different methods and datasets give different opinions. As described by Qi et al. (2014), there are eight water masses in summer and only five in winter in the ECS. Among these, Kuroshio Surface Water (KSW), Kuroshio Intermediate Water (KIW), ECS Surface Water (ECSSW), Continental Coastal Water (CCW), and Yellow Sea Surface Water (YSSW) exist throughout the year. Kuroshio Subsurface Water

(KSSW), ECS Deep Water (ECSDW), and Yellow Sea Bottom Water (YSBW) are all seasonal water masses, occurring from May through October. The CCW, ECSSW and KSW all have significant seasonal variations. In addition, the CCW is affected by river runoff and ECSSW by the CCW and KSW (see Table R21-1).

Table R21-1. T-S characteristics of water masses in East China Sea (T: °C, D: m)

Water mass		February	May	August	November
Continental Coastal Water (CCW)	T	7.0–15.5	13.4–23.5	22.0–28.0	15.5–21.5
	S	30.4–32.2	28.5–32.4	27.0–31.0	29.0–32.3
	D	0–30	0–20	0–20	0–30
East China Sea Surface Water (ECSSW)	T	11.5–20.5	14.5–24.5	23.0–28.5	17.0–25.0
	S	33.5–34.4	33.2–34.2	33.0–34.0	33.4–34.2
	D	0–200	0–50	0–75	0–200
East China Sea Deep Water (ECSDW)	T		13.5–21.5	15.5–24.5	
	S		33.5–34.4	33.4–34.4	
	D		50–200	75–200	
Kuroshio Surface Water (KSW)	T	14.2–24.4	19.0–27.8	23.7–30.2	15.0–26.0
	S	34.5–34.9	34.3–34.8	34.0–34.6	34.2–34.8
	D	0–450	0–60	0–75	0–400
Kuroshio Subsurface Water (KSSW)	T		13.0–23.3	13.0–25.0	
	S		34.6–35.0	34.5–35.0	
	D		50–400	60–400	
Kuroshio Intermediate Water (KIW)	T	7.4–13.5	6.5–13.6	7.0–13.8	6.6–13.9
	S	34.3–34.6	34.1–34.5	34.2–34.5	34.3–34.5
	D	>270	>240	>250	>280
Yellow Sea Surface Water (YSSW)	T	7.5–13.5	11.5–15.5	18.3–22.4	13.0–16.5
	S	32.5–33.6	32.0–33.2	31.5–32.4	32.0–33.4
	D	0–50	0–20	10–20	0–50
Yellow Sea Bottom Water (YSBW)	T		12.5–14.0	13.5–17.0	
	S		32.5–33.5	32.0–33.5	
	D		20–50	20–50	

Some other works have been carried out based on remote sensing data (e.g., Yuan et al., 2008) and models (e.g., Yuan and Hsueh, 2010; Yang et al., 2011; 2012). Yuan et al. (2008) studied the intrusion of the TWC into the Changjiang mouth and Subei using sea surface temperature (SST) and ocean color in winter. Yang et al. (2011, 2012) proposed an intrusion pathway of the Taiwan Warm Current Inshore Branch (TWCIB) in summer. Using remote sensing data, we can only investigate phenomena in the sea surface, which is strongly influenced by solar heating and Changjiang runoff (Figure R21-3). It is difficult to study the phenomena in lower layers. Application of a local marginal sea model depends closely on the artificial boundary conditions along the open boundary, where the vertical structures of currents and their temporal variations are difficult to set up (Guo et al., 2003, 2006). The existing T-S diagram methods of analyzing water masses are useful in open ocean water mass analysis, but it is difficult to determine the core of original water masses in a shallow sea area by these methods because a large error may be introduced.

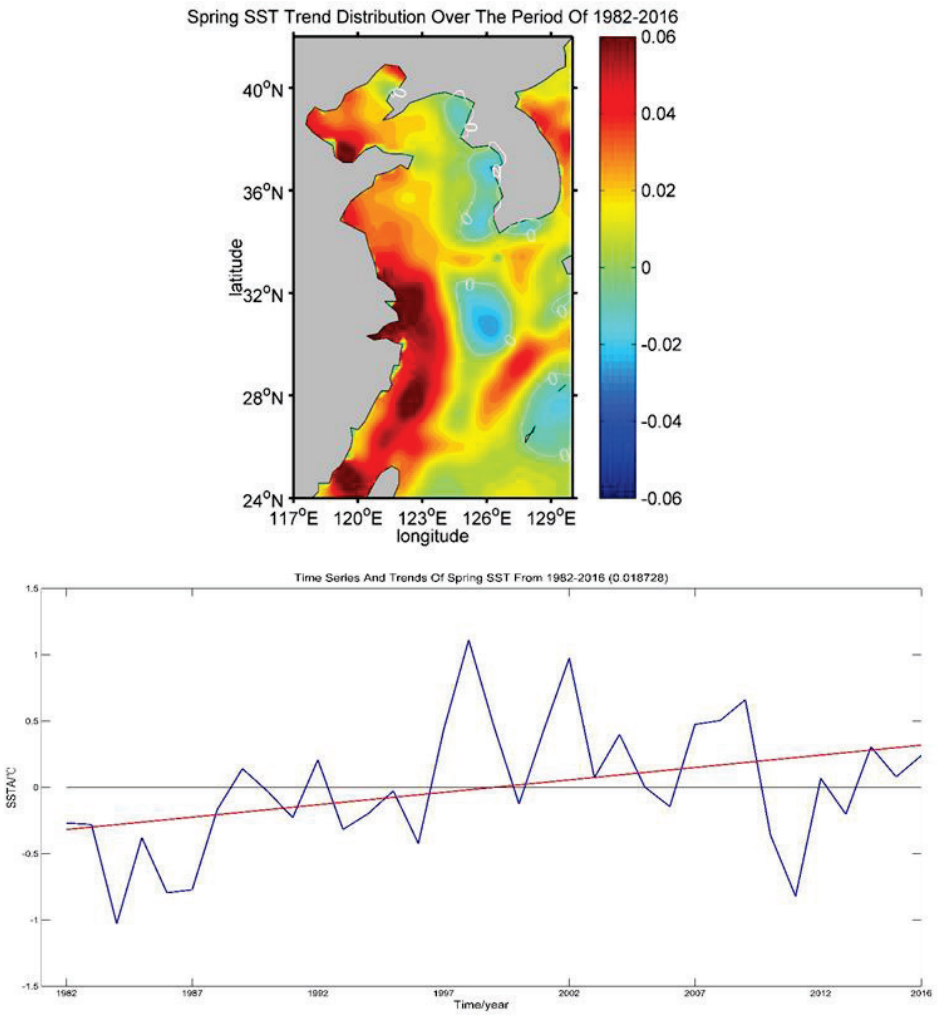

Figure R21-3. (Top) Spatial distribution of SST trend in spring from 1982 to 2016. (Bottom) Regression analysis of sea surface temperature (SST) by daily Optimum Interpolation Sea Surface Temperature (OISST) of the ECS from 1982 to 2016.

The tide plays a significant role in mixing in the ECS. With the help of a three-dimensional numerical model, the patch-like structure of low-salinity water detached from the Chanjiang Diluted Water (CDW) is demonstrated to be related with intense tide-induced vertical mixing during the spring tide (Moon et al., 2010). Yang et al. (2017) studied the tidal straining within two different stations that have different stratification environments in the East China Sea, through field observation. Their results showed that the tidal straining induces a semi-diurnal switching between stable and unstable stratification at both stations. Near-bottom high-frequency velocity measurements further revealed that the dissipation rate of turbulent kinetic energy (TKE) is highly elevated during periods when unstable stratification occurs. Further in-situ observations is needed to study the old and forever evolving subject of tidal dissipation.

Researchers have made considerable progress in the area of vertical mixing in the ECS since the 2000s. Studies have shown that vertical mixing is generally enhanced in the surface and bottom layers because of wind effects and tidal motions, but that the turbulence intensity is not always enhanced in the sub-surface layer. Various studies have suggested that the turbulence is enhanced intermittently around the pycnocline (Matsuno et al, 2006; Lozovatsky et al., 2015), perhaps because of the activities of internal waves. Shear instability associated with the breaking of internal waves might occur intermittently. Liu, Z.Y et al. (2009) found that there were large vertical variations in the eddy diffusivity K_z around the pycnocline; that is, the K_z was very small within, but was large just below the pycnocline. It is very important to note that stratification is strongly related to the distribution of the turbulence intensity, and this occurs not only around the pycnocline, but also under weak stratification in the surface mixed layer and bottom boundary layer. The relationship between the turbulence intensity and stratification is difficult to understand because stratification not only contributes to, but is also a result of, turbulent mixing. Given that the shear instability may cause enhanced turbulence, strong mixing might occur when the gradient Richardson number is small, which means the turbulence intensity should be negatively correlated with the stratification. However, as mentioned by Lozovatsky et al. (2015), even in the ECS, the turbulence intensity was positively correlated with the stratification in some cases, which suggests that it follows the parameterization of Mackinnon and Gregg (2005). The fact that the internal wave fields in the ECS were not fully developed, as expressed by the model of Garrett and Munk (1975), probably reflects various complicated boundary conditions. It would therefore be difficult to propose a universally applicable parameterization; instead, some specialized parameterizations that are specific to individual conditions would need to be developed so that the mixing processes in the ECS can be quantitatively evaluated.

Previous studies have shown that SST over the East Asian marginal seas is characterized by a strong warming trend. In addition, global warming has been thought of a key mechanism leading to such a warming trend in the ECS. However, such warming reached a peak in the late 1990s, subsequently, a basin-scale cooling has been observed in the past decade. Recent studies argue that a low frequency

variability of SST, which is associated with both the atmospheric circulation and oceanic condition, is responsible for such a cooling trend in the ECS. For example, it has been found that the SST in the ECS varied closely with the PDO before the late-1990s, indicating that the warming trend in the ECS SST was closely linked to the PDO. However, the recent SST in the ECS is largely influenced by the intensified Siberian High pressure system via enhanced heat losses in terms of latent and sensible heat fluxes. This indicates that low frequency SST variability in the ECS might be largely determined by the relative role of the atmosphere and ocean system.

A number of studies have indicated that the sea level in the ECS, including the Chinese coastline, is rising, which is closely associated with regional tidal dynamics. In addition, the interannual variability of sea level variations is associated with a large scale of SST variations in the Pacific such as the PDO. In particular, a regional ocean general circulation model simulation showed that at the end of the 21st century, the sea level in the ECS will rise about 0.12 to 0.20 m, which is mainly caused by ocean mass redistribution due to the ocean dynamic change of the Pacific Ocean (Chen et al., 2014). These results indicate that it is essential to examine the relationship of the ECS and the surrounding ocean to understand the SST and sea level variations in the ECS from the present to future.

4. Chemical Oceanography

4.1. Nutrients

The ECS receives a tremendous riverine supply of fresh water, suspended sediment and nutrients, notably from China. The salt marsh in the Changjiang Estuary plays an important ecological role in nutrient transport from the river to offshore areas, and increases P limitation (Liu et al., 2016). Eutrophication has become an overwhelming phenomenon in the coastal environment off the Changjiang Estuary; a high level of nutrients from land sources are constrained to the inner and middle shelf region, with phosphorus as a limiting element for phytoplankton growth (Zhang, J. et al., 2007; Gao et al., 2015;), red-tide events happen frequently and hypoxia exists in near-bottom waters (Zhu et al., 2011, 2016, 2017; Liu, K.-K. et al., 2015), while the open ECS shelf and slope waters remain oligotrophic (Zhang, J. et al., 2007). Across the ECS shelf, nutrients in surface waters gradually decrease from eutrophic coastal to oligotrophic open shelf waters, and the influence of land-source nutrients can be seen at surface over a distance of up to 250–300 km from the coast (Wu et al., 2003; Ren et al., 2006;). Taiwan Current Warm Water and Kuroshio Surface Water are devoid of nutrients. The Kuroshio Subsurface Water (KSSW) is rich in nutrients, and extensive exchange of water and nutrients between the ECS and Kuroshio occurs across the shelf break region through upwelling and frontal processes and spreads over a broad part of the shelf, reaching a water depth of 50–100 m at mid-shelf (Chen et al., 1995; Chen, 1996; Gong et al., 1996; Liu et al., 2000; Zhang, J. et al., 2007). The exchange across the shelf edge with the Kuroshio is of great importance for

productive fisheries and the nutrient budget (Chen and Wang, 1999; Zhang and Su, 2006).

Nutrients in the Changjiang Estuary and the ECS show seasonal variations in terms of riverine input, biological activities, and current regime (Zhang, J. et al., 2007; Chen, 2008; Liu, S.M. et al., 2016). In summer, affected by riverine input, upwelling, and monsoons, high concentrations of nutrients cover the Changjiang Estuary and the river plume which extends towards Cheju Island, in the area southwest of Korea, and in an upwelling area northeast of Taiwan (Zhang, J. et al., 2007; Chen, 2008). In winter, cooling and strong vertical mixing result in the concentrations of nutrients generally exceeding those in summer, especially in the surface layer. Affected by the strong northeasterly monsoon, high concentrations of nutrients derived from the Changjiang flow southwestward along the southeastern coast of China (Zhang, J. et al., 2007; Chen, 2008). While the concentration of nutrients is deficient in the offshore area of the ECS, which is related to the influence of the Kuroshio and the Taiwan Warm Current intruding into the saline warm surface waters of the ECS, the Subei coastal current extends southeastward to enter the northern ECS, with low discharge and a prevailing northeasterly wind (Wang et al., 2003; Chen, 2008). In spring and fall, spatial variations of nutrients are subject to transitions between summer and winter.

Shiozaki et al. (2010) reported that there was a patch of higher abundance of N_2-fixing filamentous diazotrophs, *Trichodesmium* spp., in the surface water of the ECS and Kuroshio region, and the median N_2 fixation activity at the observed stations was about 3.0 nmol N L^{-1} d^{-1}, with an order of higher values at several locations (i.e., 14 or 28 nmol N L^{-1} d^{-1}). Unicellular diazotrophic cyanobacteria such as UCYN-A are also major agents to carry out N_2 fixation, and their activity in the Kuroshio-influenced ECS area is equal to or greater than that of *Trichodesmium* and diatom–diazotroph associations containing the cyanobiont (Wu et al., 2018). Because *Trichodesmium* is capable of hydrolyzing dissolved organic phosphorus (DOP) compounds as phosphorus sources (Mulholland et al., 2002) as well as many ofthe phytoplankton species, the bloom of these N_2-fixing cyanobacteria can become additional nutrient (dissolved inorganic nitrogen, DIN and dissolved inorganic phosphorus, DIP) sources for other microorganisms through biological decomposition.

In the ECS, the DOP concentration generally exceeded the DIP concentration in the surface layer (<100 m) of the outer shelf, while DIP is the major form of dissolved P, accounting for more than 70% of the total dissolved phosphorus pool in inner and middle shelf waters (Fang, 2004). Because excess nitrogen supplies to the surface water of the ECS have occurred due to increasing atmospheric deposition (Kim et al., 2011) and terrestrial input (Liu, S.M. et al., 2016), the availability of DOP is an essential factor to consider nutrients supplies supporting primary production at offshore waters. Because one of the DOP components, phosphomonoesters, is hydrolyzed into phosphate by an extracellular enzyme, alkaline phosphatase (AP), this activity (APA) has been used to check whether microphytoplankton experience phosphorus stress (e.g., Dyhrman and Ruttenberg, 2006). APA is very low at the upwelling zone where DIP is supplied from deeper layers, while APA is enhanced at

DIP-depleted at surface Kuroshio waters (Liu et al., 2010), suggesting potential use of DOP as a nutrient supply.

Typhoon-induced mixing is an important physical factor to lift up nutrients from the subsurface layer to surface waters. Typhoon passages crossing the shelf-slope push the Kuroshio current axis shelfward and lead to the upwelling and vertical mixing of subsurface Kuroshio water with plenty of nutrients, in addition to enhancing input of nutrient-replete terrestrial waters. Hung et al. (2013) reported that nitrate and phosphate supplies to the water column in the southern ECS after the typhoon's passage were 5.6×10^{11} g-N day^{-1} and 7.8×10^{10} g-P day^{-1}, respectively, which were significantly higher than those before the typhoon occurred (nitrate supply = 1×10^{9} g-N day^{-1}, phosphate supply = 1.6×10^{8} g-P day^{-1}), which account for approximately 86% and 87% of summer nitrate and phosphate supplies, respectively, to the southern ECS. Enhanced phytoplankton chlorophyll-a and primary productivity (Siswanto et al., 2008b, 2009; Hung et al., 2013) and sinking particulate organic carbon (POC) fluxes (Hung et al., 2010) were observed after the typhoon passages.

Nutrient budgetary calculation for the ECS differs from previous LOICZ (Land-Ocean Interactions in the Coastal Zone) procedures (Gordon et al., 1996) because the limited data sets from the ECS do not allow specification of the "mixing terms" for water channels/straits and/or at the open boundary (Zhang, J. et al., 2007). Nutrient budgets were first built for the ECS by Chen and Wang (1999). The revised budgets take into account monitoring and field observation data for river inputs, atmospheric dry and wet depositions, and sediment–water interface exchange fluxes, and separated nitrate and ammonium (Figure R21-4). The results of the revised budgets suggest that the ECS shelf does not likely export substantial amounts of dissolved nutrients to the open Northwest Pacific Ocean (Zhang, J. et al., 2007).

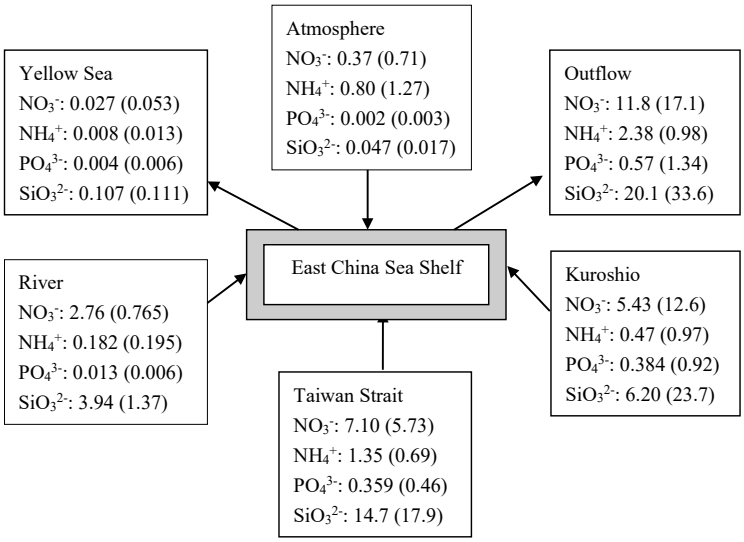

Figure R21-4. Box model showing the nutrient budgets of the East China Sea Shelf, including the nutrient fluxes (kmol s^{-1}) in summer and winter (in brackets), respectively.

Based on monitoring observations in the lower reaches of the Changjiang River, Li et al. (2007) indicated that concentrations and fluxes of DIN and phosphate had increased greatly since the 1950s, while annual average concentration and flux of dissolved silicate had an opposite trend, showing a sharp decrease since the 1950s. They stated that fertilizer application peaking after the 1980s could be responsible for the high DIN and DIP levels, and construction of dams could be linked to the decrease of dissolved silica. Based on historical summertime data from 1959 to 2009, Jiang et al. (2014) reported similar results for the concentrations of nitrate, nitrite, ammonium, and phosphate and ratios of N/P and N/Si in the freshwater and saline sections of the Changjiang Estuary which all increased because of persistent riverine loading, but silicate levels remained constant like previous studies (Liu et al., 2003, 2009). As a result, microalgal biomass showed a dramatic increase with a decreasing diatom–dinoflagellate ratio and exacerbated harmful algal blooms, which is closely related to an increase in anthropogenic activities and climatic changes (Jiang et al., 2014). Using historical in situ data sets from 1971 to 2001, an increase in DIN at summer surface water was also observed in the northern ECS, probably due to the combination of changes in Changjiang discharge and increase of nitrogen fertilizer use in China (Siswanto et al., 2008a). Although scientists are paying much attention to the response of the ECS ecosystem to changes in the nutrient supply arising from the Three Gorges Dam project, it is still not clear if there are any changes because of the lack of time-series data and the complex interactions in the Changjiang Estuary (Gong et al., 2006; Jiang et al., 2014).

Environmental change in the ECS slope and Kuroshio region is also not clear due to a limited data set. Based on in situ data from 1987 to 2009 in the ECS outer shelf/slope region, nitrate concentrations and nitrate flux in the Kuroshio were examined; Guo et al. (2012) indicated that the nitrate concentration in the middle and bottom layers across the Kuroshio was found to increase significantly over the 23-year period, especially after 2004, while nutrient transport did not increase significantly due to decreased current velocity.

4.2. Hypoxia

Due to the monsoon season, hypoxia in the ECS usually occurs in summer (usually in August), whereas in winter oxygen depletion in the near-bottom waters is usually alleviated due to strong mixing (Lim et al., 2006; Tishchenko et al., 2013; Zhu et al., 2017). Of all the reported hypoxic zones in the East China Sea, the area of most of these zones is on the order of a few hundred square kilometers (or even less). The biggest hypoxic zone is located in the region off the Changjiang Estuary adjacent to the ECS. In August 2006 it covered an area of 15,400 km^2 (Zhu et al., 2011). Though hypoxic areas can be traced back as early as in 1950s, large ones (i.e., areas over 10,000 km^2) were all found after 1999. Hence it is generally accepted that oxygen depletion has become more severe in recent decades (Chen et al., 2007; Zhu et al., 2011; Wang et al., 2012). The area of the hypoxic zone was first reported as 1900 km^2

(Office of Integrated Oceanographic Survey of China, 1961). In the 1980s, it was hard to derive its area, which was conservatively estimated as smaller than the area found in the 1950s (Figure R21-5b). As shown in Figure R21-5b, after the 1990s the hypoxic area became much larger. In 1999, it was found to be 13,700 km^2 (Li et al., 2002), 15,400 km^2 in 2006 (Zhu et al., 2011), and 11,150 km^2 in 2013 (Zhu et al., 2017), respectively. These three hypoxia events are, so far, the largest events that have ever been found. In the three big hypoxia events (i.e., hypoxia in 1999, 2006 and 2013, the same hereafter), oxygen depletion was estimated as 4.7, 7.2 and 5.1 million tons, respectively (Zhu et al., 2017).

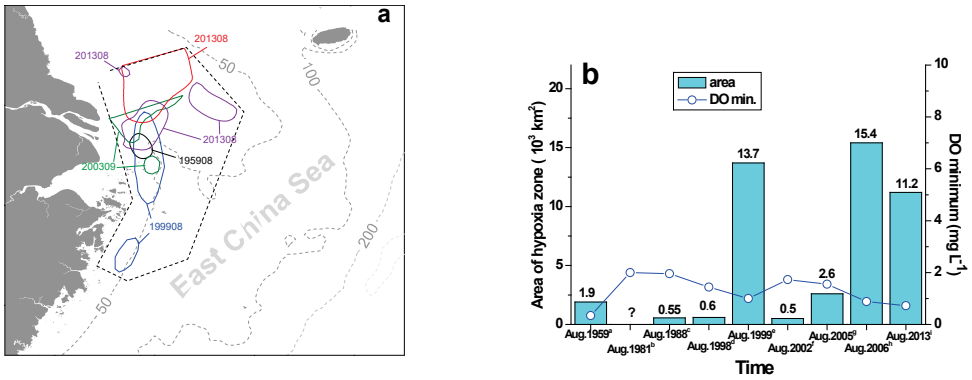

Figure R21-5. Pooled key hypoxia zone of its a) locations and b) areas in the region off the Changjiang Estuary and adjacent ECS. Plots after Zhu et al. (2011); a: Office of Integrated Oceanographic Survey of China (1961), b: Limeburner et al. (1983), c: Tian et al. (1993), d: Wang and Wang (2007), e: Li et al. (2002), f: Wang (2009), g: Zhu, Z.Y., unpublished data, h: Zhu et al. (2011), i: Zhu et al. (2017)).

With respect to the second factor, namely the biogeochemical process that consumes dissolved oxygen in the waters, due to strong anthropogenic activity, the Changjiang River nutrient flux has been found to be increasing in the past decades (Zhang et al., 1999) and eutrophication is hence suggested to play an more important role in the estuarine region and adjacent ECS (Wang, 2006). In addition to the trend in eutrophication in recent decades, sediment core studies further imply that the marginal sea has been under a mild eutrophication over the past hundred years (Zhu et al., 2014). Elevated terrestrial materials input from the Changjiang River (and a minor contribution from the small rivers along Zhejiang province) into the estuarine zone and adjacent ECS promotes the in situ production. Indeed, blooms become common from May to August in the region off the Changjiang Estuary and adjacent ECS (Zhu et al., 1997). Vigorous primary production in the upper layer generates excess organic matter, part of which sinks to the bottom layer where it finally decays. In the vicinity of the Changjiang River mouth, terrestrial organic matter may be an important source of decaying organic matter in the bottom waters that consumes bottom dissolved oxygen. However, the majority of the decaying organic matter in this

region (i.e., where hypoxia is frequently found) is thought to be of marine origin.

Overall, hypoxia in the ECS is understudied when compared to other large coastal hypoxia regions like the central Baltic Sea and the Gulf of Mexico. For example, hypoxia and its feedback to the ecosystem via nutrient modification remains largely unknown, while in the Baltic Sea it is clear that hypoxia alleviates phosphate limitation, promotes further phytoplankton blooms and hence enhances further hypoxia occurrence (Zilius et al., 2014). Also, whether the hypoxia is highly related to terrestrial output seems more complex when compared to the case in the Gulf of Mexico, where a simple relation was found between terrestrial nitrogen flux and the following bottom hypoxia (Turner et al., 2012). Another important puzzle is the role of sub-ground marine water discharge in bottom hypoxia; yet we know very little in this aspect.

4.3. Methane and nitrous oxide

CH_4 concentrations in the ECS have obvious spatial and seasonal variability due to the complex mixing of different water masses and other variables. Maximum CH_4 concentrations, sea–air and sediment–water fluxes all occur during summer. CH_4 concentration decrease gradually from the coastal area to the open sea, and high levels of CH_4 generally appear near the Changjiang Estuary and outside the Hangzhou Bay (Zhang et al., 2004; 2008a,b; Sun et al., 2018). In early spring and winter, CH_4 in the shelf region has a uniform distribution from the surface to the bottom, while it increases gradually with depth in other seasons. Horizontally, CH_4 in the surface water (usually 2–5 nM) shows a gradient from onshore to offshore, where the Changjiang River enters the ECS with abundant CH_4 and the Kuroshio intrudes onto the shelf with poor CH_4 (Zhang et al., 2004; 2008a,b; Sun et al., 2018). Vertically, three patterns can be generally summarized to differentiate the depth profile of CH_4 in the ECS, i.e., with or without the thermocline at the shelf region and deep water at the slope. The first two patterns are usually present in the shallow shelf regions near the coast, where the wind and land-source inputs strongly influence the shelf. In summer and autumn, the water column is well-stratified, resulting in the CH_4 accumulation in the bottom water due to sedimentary release. In winter and early spring, however, the water column is well mixed and the absence of the thermocline in most regions of ECS supports the diffusion of CH_4 from bottom to surface water and finally its release to the air. Hence CH_4 distribution is vertically uniform in the continental shelf zone in spring and winter. The third pattern is usually present in the deep water, such as the edge of the shelf or the slope. It is similar to the vertical distribution of CH_4 in the pelagic zone because those areas are far from land and mainly influenced by the Kuroshio. Specifically, CH_4 in the first 100 m is uniform but then reach a subsurface maximum in the next 100 m. Below the peak, CH_4 decreases with depth and stabilizes at the lowest level (~1.0-1.5 nM). Research has shown that high CH_4 is also found at the edge of the continental shelf, where the organic matter flows from the coastal to the oceanic zone and accumulates in the break areas.

N_2O concentrations showed an offshore decreasing trend in surface distribution, and a surface-to-bottom increasing gradient in water column (Zhang et al., 2008a; Wang et al., 2016). The surface N_2O concentration is highest in summer, followed by fall, and the lowest usually in early spring. The distribution of N_2O in the ECS is influenced mainly by water temperature, mixing of water masses, and biological production. N_2O concentrations showed negative correlation with temperature, but positive one with suspended particulate matter concentration. There is no specific overall correlation observed between salinity and N_2O concentration, but a coupled increasing trend within salinity range of 0–2 and a decreasing trend within salinity range of 2–30 at the Changjiang River estuary (Wang et al., 2016). Nitrification is considered to be the main process that controls N_2O production. Obvious bottom-water hypoxia occurs in the northern ECS in summer, where the nitrification and denitrification processes and the production of N_2O are expected to be enhanced, but only a slight increase of N_2O concentration has been found. The frequent vertical mixing of the water column prevents accumulation of N_2O in the bottom waters to significant high levels and may lead to more emission of N_2O to the atmosphere (Wang et al., 2016).

Although previous research has given us a glimpse of CH_4 and N_2O cycling in the ECS, we are still far from understanding the seasonal variations of CH_4 and N_2O distribution and emission, and quantifying CH_4 and N_2O sources and sinks in these areas. Most studies have been based on discrete sampling and conducted at large sampling intervals with coarsely spatial resolution. In order to obtain high-quality data to evaluate the role of the ECS in the global ocean, continuous measurements with high temporal and spatial resolution are needed. Another prospect in the future study is the biological production processes of CH_4 and N_2O in seawater. The budget of CH_4 and N_2O in the ECS remains a puzzle because the contribution of microbial processes (i.e. nitrification, denitrification and nitrifier denitrification) is still ambiguous. The explanation of the “oceanic methane paradox” is a hot topic, and aerobic CH_4 production in oxygenated water has been gradually revealed in recent studies. The relative importance of the microbial processes leading to the production and consumption of N_2O in the ECS still remains unclear. The isotopic composition of N_2O has been used to characterize local production and consumption mechanisms of dissolved N_2O in marine environments. Hopefully, new techniques (such as isotopes) may help us make progress on this in the future. Thus more studies on CH_4 and N2O in coastal and shelf waters of ECS are still needed to further add to the global oceanic CH_4 and N_2O database, and to understand the biogeochemical cycle of CH_4 and N_2O in the shelf areas and their regional contribution to global oceanic CH_4 and N_2O emission.

4.4. Biogeochemical tracers

Trace elements and their isotopes (TEIs) are key parameters of GEOTRACES program. Many trace elements (e.g., Fe, Co, Cu) are micronutrients that play critical roles in the ocean ecosystem and therefore control the structure and productivity of

marine ecosystems as well as carbon cycling. Other trace elements and isotopes can be used to assess ocean processes. For example, Al, Mn, rare earth elements (REEs; Zhang et al., 2018), $^{143}Nd/^{144}Nd$, and Ra isotopes have been used to identify and quantify mixing of various water masses, including riverine input and submarine groundwater discharge. Given the crucial importance for TEls and isotopes serving as biogeochemical tracers, knowledge of their processes and fluxes which control their distribution and internal cycling is required.

The distribution of dissolved aluminum (Al) in the Changjiang Estuary and ECS was reported as early as 1984 by Mackin and Aller (1984). Dissolved Al in the Changjiang Estuary varies widely (18–200 nmol L^{-1}) at very low salinity, but seems to be constant when the salinity is between 1 and 30 (Ren et al., 2005). The concentration of dissolved Al generally decreases gradually from the Changjiang Estuary to the central shelf, and then decreases sharply at the shelf break. Dissolved Al ranges from 2.4 to 112.6 nmol L^{-1} on the shelf (Minakawa and Watanabe, 1998; Ren et al., 2006, 2015). The average residence time of dissolved Al is 339 ± 118 days (Ren et al., 2006). Ren et al. (2015) calculated the cross-shelf transport of Al flux at the subsurface layer and found that the coastal-enriched Al water was mainly exported to Region 19 or western Pacific Ocean.

Dissolved manganese (Mn) concentrations in the ECS range from 1.5 to 140.7 nmol L^{-1} , with an average of 8.2 nmol L^{-1} . Seasonal variations of dissolved Mn in the ECS are significant, with the highest concentrations occurring in summer with maximum concentrations (140.7 nmol L^{-1}) occurring in near-bottom waters of the suboxic zone. Extensive consumption of oxygen results in the regeneration of dissolved Mn in near-bottom waters of the suboxic zone (Wang et al., 2016). Dissolved Mn in the Changjiang Estuary behaves nonconservatively, and is removed significantly by net sorption onto suspended particles. The concentration of dissolved Mn decreases with distance from the coast across the ECS. Mn-rich ECS shelf waters are exported to the Kuroshio waters, and have the potential to influence the northwestern Pacific Ocean as well as Region 19. The estimated average residence time for dissolved Mn is 76 to 350 days in the ECS (Wang et al., 2016).

The average concentration of total dissolved iron (D-Fe) in the surface water of the Changjiang River estuary in spring and autumn is 39.4 ± 26.6 nmol L^{-1} and 20.5 ± 11.0 nmol L^{-1} , respectively. The average bottom D-Fe concentrations in the estuary in spring and autumn is 76.1 ± 58.6 nmol L^{-1} and 78.5 ± 39.0 nmol L^{-1} , respectively. The average D-Fe concentration in both surface and bottom waters in spring is higher than that in autumn. The average surface concentration of Fe organic ligands (Lt) in the estuary in spring is greater than that in autumn (40.0 ± 26.8 vs 23.2 ± 7.8 nmol L^{-1}). Both D-Fe and Lt are elevated in the Changjiang River estuary and the Hangzhou Bay, but depleted with distance offshore of the ECS (Su et al., 2015). Dissolved Fe is significantly correlated with Lt and the limitation of total dissolved phosphate (TDP) decreases the uptake of Fe (Su et al., 2017).

In the coastal waters of the ECS, the average concentrations of dissolved zinc (Zn), copper (Cu), cobalt (Co) and vanadium (V) are 14.4 ± 9.0, 22.6 ± 5.4, 0.94 ± 0.18 and 20.4 ± 5.6 nmol L^{-1} , respectively (Su et al., 2017). TDP is associated with dissolved Fe, Cu, Zn and Co, but not with V. Su et al. (2017) highlight that the limitation of TDP decreases the uptake of Fe.

5. Phytoplankton

Recently, as many red tide events are happening in the ECS, more attentions is being paid to the ecosystem and phytoplankton in this area and their relationship to human activities and climate change. Phytoplankton abundance is often expressed by the photosynthetic pigment, chlorophyll-a. Because of the complex and large variability of chlorophyll-a in this area recently, satellite ocean color data are often used to understand the over-all structures. Ning et al. (1998) and Tang et al. (1998) were the pioneers to describe satellite-derived phytoplankton abundance in this area in combination with satellite sea surface temperature (SST). Using Coastal Zone Color Scanner (CZCS) phytoplankton pigments (chlorophyll-a and pheopigments) data from 1978 to 1986, they clearly showed various water mass structures and associated phytoplankton distributions, especially the extension of high phytoplankton-rich water from the Changjiang Estuary to the offshore. However, ocean color remote sensing data overestimate chlorophyll-a near the coast because of the high amount of sediments near the coast (Kiyomoto et al., 2001) and high amount of colored dissolved organic matter from river discharge (Gong, 2004) as well as the problem of atmospheric correction (Shi and Wang, 2009).

Knowing the presence of errors in ocean color data, Yamaguchi et al. (2012, 2013) described seasonal variation of NASA ocean color sensor SeaWiFS chlorophyll-a in the ECS from January 1997 to December 2006 with standard product and locally tuned product, respectively. (Figure R21-6). They recognized the overestimation of the satellite chlorophyll-a data caused by suspended matter near the coast as well as on the Changiiang Bank during winter. They reported a spring bloom in large parts of these areas; however, the summer maximum of chlorophyll-a was also seen from the Changjiang Estuary to near the east of Jeju Island from July to September. The summer maximum shifts eastward coinciding with the movement of the Changjiang Diluted Water (CDW), taking approximately 2 months to move from the Changjiang River mouth to around Jeju Island. Yamaguchi et al. (2012) also reported that the summer chlorophyll-a was positively correlated with Changjiang River discharge with a time lag of 0 to 2 months between 1998 and 2006, and they showed that Changjiang River discharge is one of the most important factors for the interannual variation of chlorophyll-a in the middle ECS. Yamaguchi et al. (2013) found relatively low chlorophyll-a with high suspended matter near the coast and Changjiang Bank in winter (Figure R21-7). The high suspended matter decreases in spring to summer in the offshore area, and phytoplankton increase with the decrease; a spring bloom can be seen covering a large area, indicating suspended matter is important for phytoplankton dynamics in shallow areas.

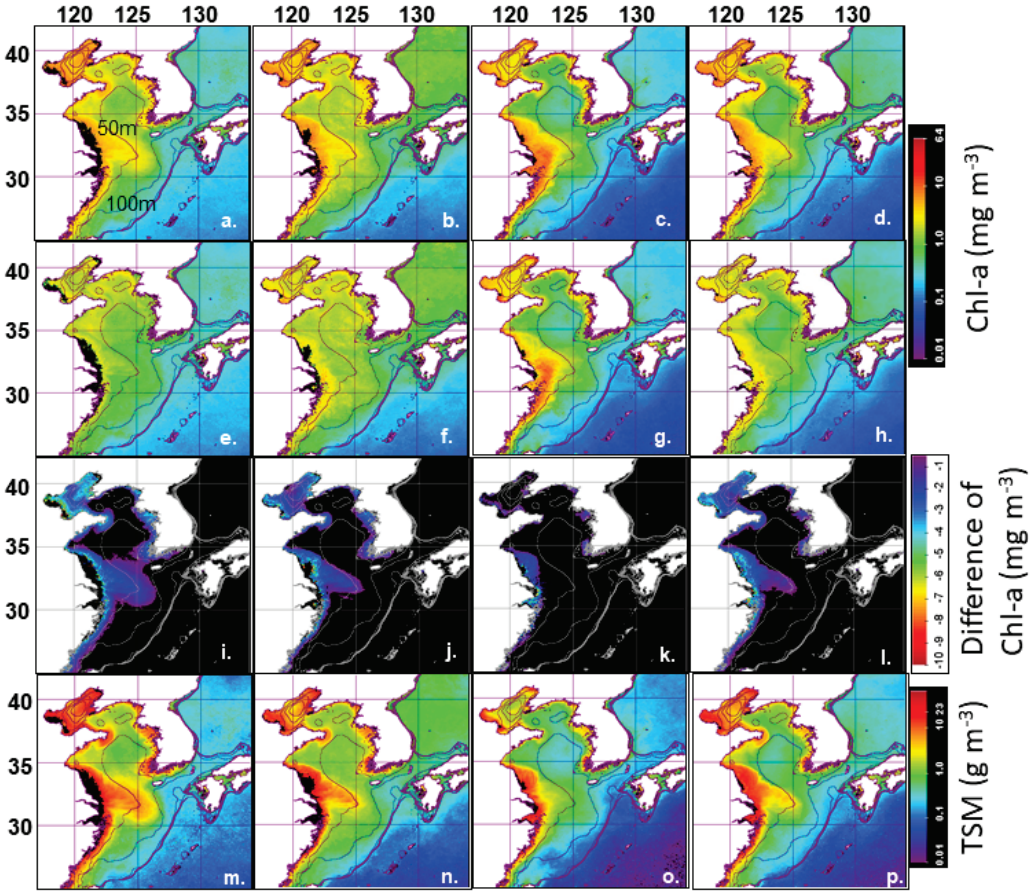

Figure R21-6. Distribution of 10-year (1997– 2006) average of monthly chlorophyll-a (chlorophyll-a; mg m^{-3}) from (a-d) standard MODIS algorithm and (e-h) from local YOC algorithm, (i-l) the difference between the two (chlorophyll-a, mg m^{-3}), and (m-p) total suspended matter (TSM; g m^{-3}) with bathymetry. (a, e, i, m) January, (b, f, j, n) April, (c, g, k, o) July, and (d, h, l, p) October. Redrawn from (Yamaguchi et al., 2013).

Yamaguchi et al. (2013) further suggested that the increase in summer chlorophyll-a over the last 10 years is possibly caused by eutrophication. In addition, Xu et al. (2013) analyzed bloom conditions in this area with a 13-year time series from SeaWiFS to MODIS to understand the relation of phytoplankton blooms to giant jellyfish blooms. The Northwest Pacific Action Plan (NOWPAP) of the United Nations Environment Programme (UNEP) has used changes of chlorophyll-a concentrations over time to monitor eutrophication in this area.

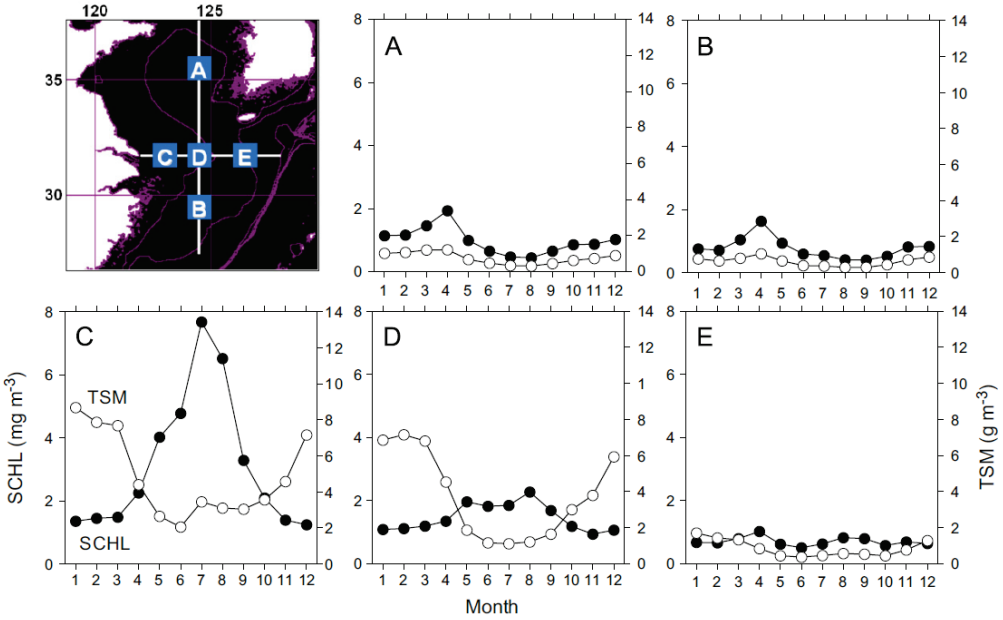

Figure R21-7. Seasonal variation in10-year (1998–2007) averaged monthly satellite chlorophyll-a (SCHL; mg m^{-3}) and total suspended matter (TSM; g m^{-3}) from January to December in (A) the middle of the Yellow Sea, (B) south of the Changjiang Bank, (C) offshore of the Changjiang River mouth, (D) around the Changjiang Bank, and (E) east of the Changjiang Bank. Black and white symbols indicate CHL and TSM, respectively. From Yamaguchi et al. (2013).

Over the ECS shelf from the Changjiang River to the shelf slope, nutrient concentrations and composition have changed differently. Based on monitoring in the lower reach of Changjiang, Li et al. (2007) indicated that concentrations and fluxes of dissolved inorganic nitrogen (DIN) and phosphate had increased greatly since the 1950s, while the annual average concentration and flux of dissolved silicate had an opposite trend, showing a sharp decrease since the 1950s. They stated that fertilizer application peaking after the 1980s could be responsible the high DIN and dissolved inorganic phosphate (DIP) levels, and constructions of dams could be linked to the decrease in dissolved silica. Based on historical summertime data from 1959 to 2009, Jiang et al. (2014) reported similar results for the concentrations of nitrate, nitrite, ammonium, and phosphate and ratios of N/P and N/Si in the freshwater and saline sections of the Changjiang Estuary, which all increased because of persistent riverine loading, but silicate levels remained constant like in previous studies (Liu et al., 2003, 2009). As a result, microalgal biomass showed a dramatic increase with a decreasing diatom–dinoflagellate ratio and exacerbated harmful algal blooms, which is closely related to an increase in anthropogenic activities and climatic change (Jiang et al., 2014). Using historical in situ data sets from 1971 to 2001, an increase in DIN at summer surface water was also observed in the northern ECS, probably due to a combination of changes in Changjiang discharge and increase of nitrogen fertilizer use in China (Siswanto et al., 2008a). Although scientists are paying much attention to

the response of the ECS ecosystem to changes in the nutrient supply arising from the Three Gorges Dam project, it is still not clear if there are any changes because of the lack of time-series data and the complex interactions in the Changjiang Estuary (Gong et al., 2006; Jiang et al., 2014).

Environmental change in the ECS slope and Kuroshio region is also not clear due to a limited data set. Based on in situ data from 1987 to 2009 in the ECS outer shelf/slope region, nitrate concentrations and nitrate flux in the Kuroshio were examined; Guo et al. (2012) indicated that the nitrate concentration in the middle and bottom layers across the Kuroshio was found to increase significantly over the 23-year period especially after 2004, while nutrient transport did not increase significantly due to decreased current velocity.

6. Zooplankton

In the ECS, Changjiang River Diluted Water (CDW) forms a typical estuarine zooplankton community (Zhang et al., 2005). Freshwater species, represented by *Brachionus falcatus*, *B. calyciflorus*, *Sinocalanus dorrii*, *Mesocycolops leuckarti* and *Thermocyctops taihokuensis*, occupy regions with salinity lower than 2. Between 122–122.5°E, where salinity ranges from 2 to 10, the zooplankton community is dominated by *Tortanus vermiculus*, *Schmackeria poplesis* and *Monoculodes limnophilus*. In the plume region with salinity of 10–25, common coastal species are dominant, including *Labidocera euchaeta*, *Sagitta nagae*, *Pseudeuphausia sinica* and *Acanthomysis sinensis*. Oceanic species are comparatively scarce around the estuary, and the occurrence of *Sagitta enflata* and *C. sincus* has been noted as a result of their exchange with open waters.

As transportation of estuarine species into the oceanic environment is difficult to detect, the ecological impacts of CDW on zooplankton has been recorded mainly as cascading effects through increased nutrient input and thereafter primary production.

The Kuroshio Current (KC) is a warm current (24°C in annual average sea surface temperature) carrying nutrient-rich waters. Confirmation of the Nearshore Kuroshio Branch Current has stimulated much research interest in China, as it can at least partially explain the observed phosphate-rich bottom water off the coast of Zhejiang province (Yang et al., 2012). Phosphate limitation has been proposed as the main reason for the occurrence of a massive dinoflagellate bloom in this region (Li et al., 2009).

However, KC-driven changes in zooplankton assemblage have been detected mostly in the south of the ECS. Both copepods and jellyfish are used as indicator species of the KC. Meanwhile, the KC has been known to transport tropical or subtropical species to water bodies on both the eastern and western sides of Taiwan Island, as it can flow northward through the continental shelf break northeast of Taiwan and the Luzon Strait into the Taiwan Strait.

The intrusion of warm water into the central ECS and north of it has been shown by the interaction between neritic and warm water tintinnids in the surface waters (Li et al., 2016). Warm water genera can reach the coast of Zhejiang province. Consistent with the seasonal change in KC strength, the largest coverage of warm water genera has been observed in August and October, compared to May (Figure R21-8). In May and August, neritic and warm-water genera are completely separated in geographical distribution, whereas their pioneer genera overlap in geographical coverage in October.

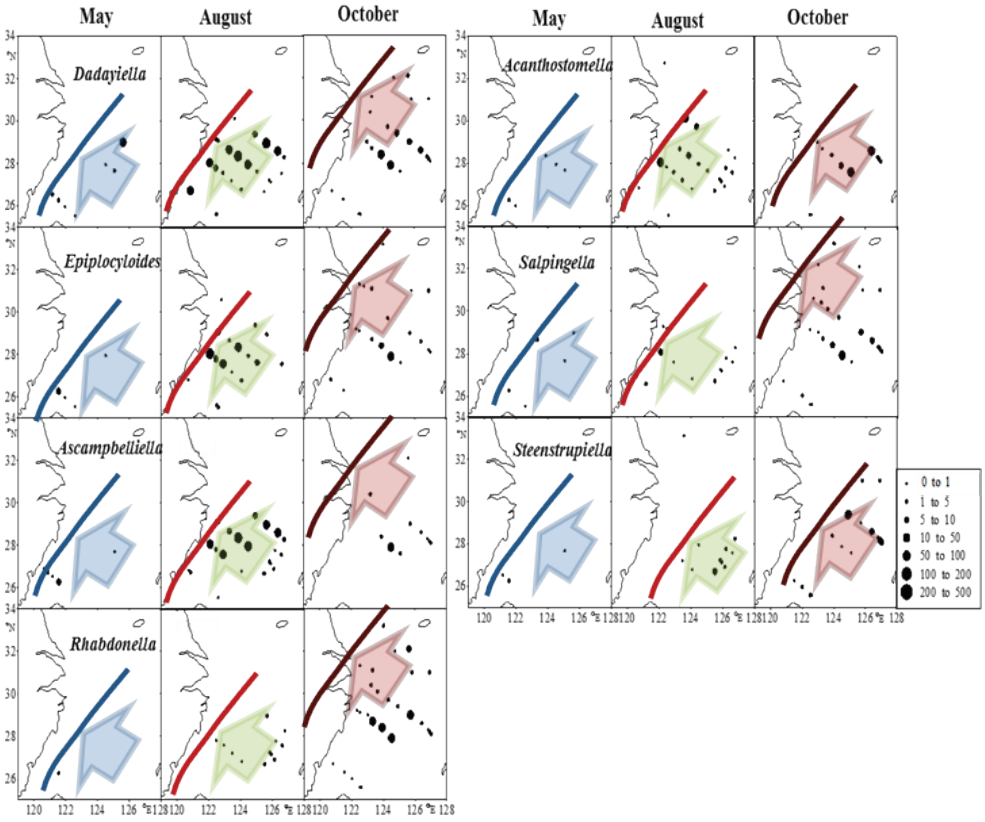

Figure R21-8. Intrusion of the Kuroshio Current into the ECS indicated by the distribution of warm-water tintinnid genera. Colored lines and arrows denote boundary and direction of the warm water intrusion, respectively. Redrawn from Li et al. (2016).

The function of zooplankton in the marine ecosystem is well understood, but it is still hard to integrate them into a numerical ecological model. The obstacles lie mostly in quantification of critical parameters, such as feeding pressure on phytoplankton and mortality caused by predation and natural death.

Potential responses to climate change and anthropogenic stresses depend critically on time series. To establish long-term observation plans and free access to existing data are important steps towards resolution of such scientific questions.

7. MacroBenthos

The East China Sea has a diverse contribution of macrobenthos species. It shares 209 species with the Yellow Sea, among which there were 139 species of Polychaeta, 31 Mollusca, 18 Crustacea, 16 Echinodermata and 5 species in other groups. The species composition of macrobenthos in the ECS has seasonal variations, with the ranking of species numbers being spring (452 species) > autumn (435) > summer (380) > winter (288) (Li, 2003)

Figure R21-9 shows the seasonal distribution pattern of macrobenthic species numbers in the ECS. In spring, a large number of species was found in the southern and northern areas of the ECS and the northern area of the Taiwan Strait, but in the middle area of the ECS, the number was low (Li, 2003). In summer, a high number of species was found in the middle and northern areas of the ECS and the northern area of the Taiwan Strait. In autumn, the middle and northeastern areas showed high species numbers, but numbers in the southern area was low. In winter, the distribution of species numbers was relatively homogenous.

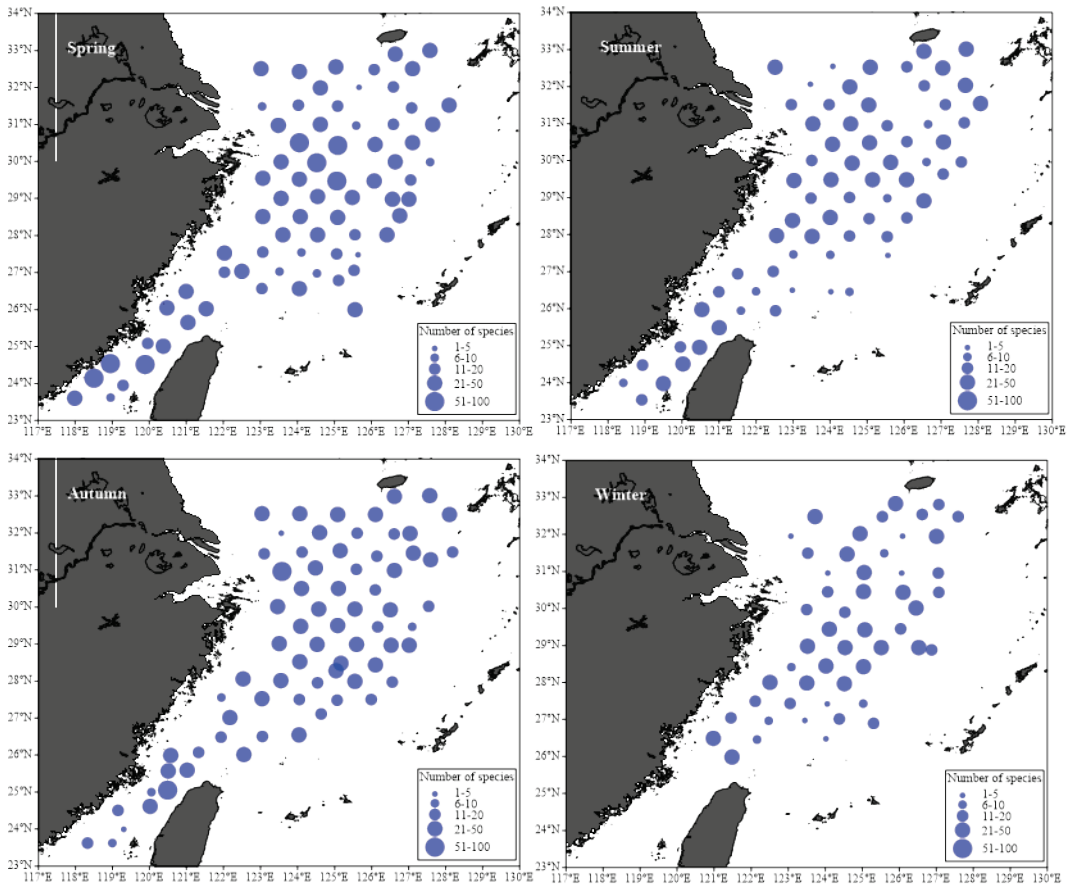

Figure R21-9. The distribution pattern of macrobenthic species numbers in the East China Sea. From Li (2003).

During 2006 and 2007, in the project “the second Chinese National Ocean Census”, 1300 macrobenthic species were recorded in the ECS, including 428 species of Polychaeta, 291 Mollusca, 283 Crustacea, 80 Echinodermata, and 218 species in other groups (Sun, 2012). Seasonal variation in species numbers of macrobenthos showed higher values in summer and winter and lower values in spring and autumn. In the sea adjacent to Changjiang River estuary, the area off the Zhejiang coast and the Taiwan Strait, the number of species was 418, 327 and 492, respectively, with Polychaeta being the dominant taxonomic group. The spatial distributions of different dominant species were also different among the dominant species. The dominant macrobenthic species are listed in Table R21-2.

Table R21-2. Dominant microbenthic species in the East China Sea from 1997 to 2000 (Li, 2003).

Taxonomic group	**Dominant species**	**Taxonomic group**	**Dominant species**
Polychaeta	*Paralacydonia paradoxa*	Mollusca	*Dentalium octangulatum*
	Sigambra hanaokai		*Bursa rana*
	Goniada maculata		*Mitrella burchardi*
	Glycera sp.		*Nassarius siquijorensis*
	Glycera chirori		*Zeuxis* sp.
	Prionospio malmgreni		*Inquisitor flavidula*
	Prionospio pygmaea		*Lophiotoma leucotropis*
	Paraprionospio pinnata	Crustacea	*Ampelisca cyclops*
	Paraprionospio sp.		*Ampelisca miharaensis*
	Lumbrineris latreilli		*Eriopisella sechellensis*
	Magelona sp.		*Leptochela acculeocaudata*
	Notomastus aberans		*Alpheus distinguendus*
	Onuphis eremita		*Callianassa japonica*
	Aglaophamus dibranchis		*Jassa falcata*
	Aricidea fragilis		*Byblis japonicus*
Mollusca	*Angulus lanceolatus*		*Grandidierella japonica*
	Spiniplicatula muricata	Echinodermata	*Amphioplus laevis*
	Episiphon kiaochowwanensis		*Amphioplus depressus*
	Graptacme buccinulum		*Amphioplus ancistrotus*
	Calliodentalium crocinum		*Amphiura vadicola*
	Solen canaliculatus		*Amphiura digitula*
	Olivella sp.		*Ophiura kinbergi*

During 2006 and 2007, in the second Chinese National Ocean Census project, researchers found that some dominant species in the sea adjacent to the Changjiang River estuary, the area off the Zhejiang coast and the Taiwan Strait had similar distributions, while species in the other groups had different distributions. *Sternaspis scutata* and Nemertinea were highly dominant in all three areas (Sun, 2012).The mean abundance of macrobenthos in the ECS was 280 ind./m^2, among which Polychaeta showed the highest abundance, followed by Crustacea and Mollusca. The seasonal variation of macrobenthic abundance was autumn (461 ind./m^2) > spring (336 ind./m^2) > summer (178 ind./m^2) > winter (146 ind./m^2).

The spatial distribution pattern of macrobenthic abundance showed that high abundance existed in the inshore area and low abundance in the offshore area. There were also obvious seasonal and latitudinal patterns for abundance. In spring, the abundance was high in the middle area of the ECS, the inshore area of the Changjiang River estuary, and north of the Taiwan Strait, with the highest value reaching 1000 ind./m^2, showing a decreasing trend from inshore to offshore. In summer, there were two high abundance areas. One was located in the inshore area of the estuary and the other was situated from the estuary to the north of the Taiwan Strait, both of which had the highest value of 250 ind./m^2. In autumn, the abundance in the inshore area (highest abundance was up to 1500 ind./m^2) was higher than that in the offshore area. In winter, high abundance occurred in the coastal area of Zhejiang province and in the offshore area of Hangzhou Bay, with the high abundance of 250 ind./m^2 (Li, 2003).

The spatial distribution of macrobenthic biomass also showed obvious seasonal and latitudinal patterns. In spring, the biomass was high in the inshore area of the ECS, showing a decreasing trend from inshore to offshore; the biomass had highest values (250 g/m^2) in the coastal area of Zhejiang province and formed high value areas in the north and middle of the Taiwan Strait. In summer, the biomass was lower than that in spring; high biomass areas were located in the middle area of the Changjiang River estuary and the offshore area of Hangzhou Bay, and low biomass area in the north of the Taiwan Strait. In autumn, high biomass areas were formed in the coastal areas of the estuary and Hangzhou Bay with the highest value being 150 g/m^2, and low biomass area north of the Taiwan Strait. In winter, high biomass areas were the middle area of the estuary and the inshore area of Hangzhou Bay with the highest value being 90 g/m^2. (Li, 2003).

Li (2003) classified the macrobenthos in the ECS into 5 communities: the north inshore community, north offshore community, south inshore community, south offshore community and Taiwan Strait community, respectively (Figure R21-10).

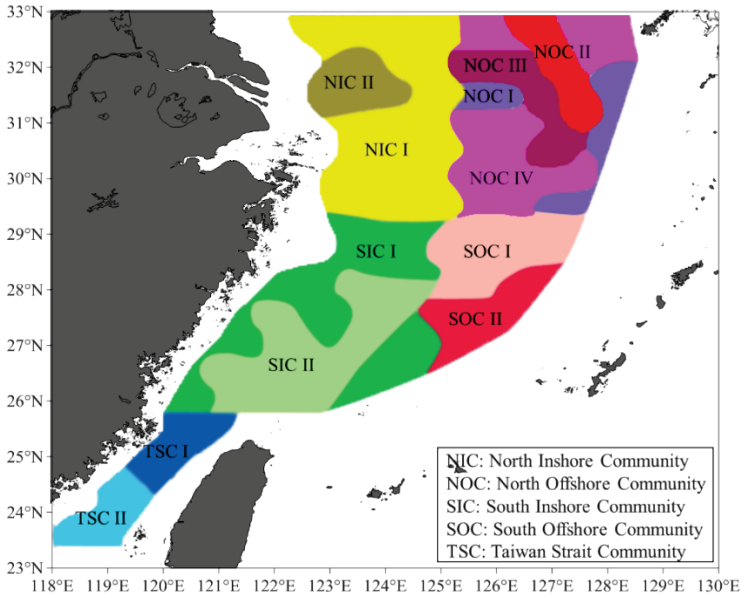

Figure R21-10. The distribution pattern of macrobenthic communities in the East China Sea from 1997 to 2000. From Li (2003).

Up to now, we still lack the long-term, large spatial-scale investigations of macrobenthos in the ECS. The forming mechanism and the variation regularity of the macrobenthic community are still short of macroscopic analysis. However, many studies have been conducted on the macrobenthic ecology and biodiversity in the ECS. A geographic information system (GIS) database has also been established. We think that in the future it is essential to conduct research in the following directions (Li, 2011).

First, data from macrobenthos investigations collected since 1956 should be gathered and integrated, and a new ecological theory and new data analyzing method should be applied to study the temporal and spatial variations of macrobenthic community structure of more than half a century, combined with environmental variables such as primary productivity, hydrology, and sediment characteristics. The relationship between macrobenthic variation and global climate variation also requires on-going research. Second, the bio-indicating function of the macrobenthic community to marine environmental pollution needs to be studied; the indicator species, dominant species and their variations over time also need to be clarified. Third, ecological models should be developed to predict the variation trends of the macrobenthic community; the role and status of macrobenthos in nutrient flow and material flow in the ecosystem and their relationship with plankton and nekton, as well as hydrology also require explanation.

8. Fish and Invertebrates

Fish community in the Changjiang River estuary includes both warm-water pelagic and cold-water demersal species, and includes both coastal species and offshore

migratory species. According to the fishery investigation in 2004, the fish community in the Changjiang River estuary included 47 species, representing 42 genera and 31 families, among which Perciformes occupied the most, including 23 species, 21 genera and 15 species (Figure R21-11). Fish community composition showed seasonal variation in the estuary, with the common feature that the community was comprised mainly by Perciformes (Figure R21-12). All fish species and their occurrence in different months are listed in Table R21-3.

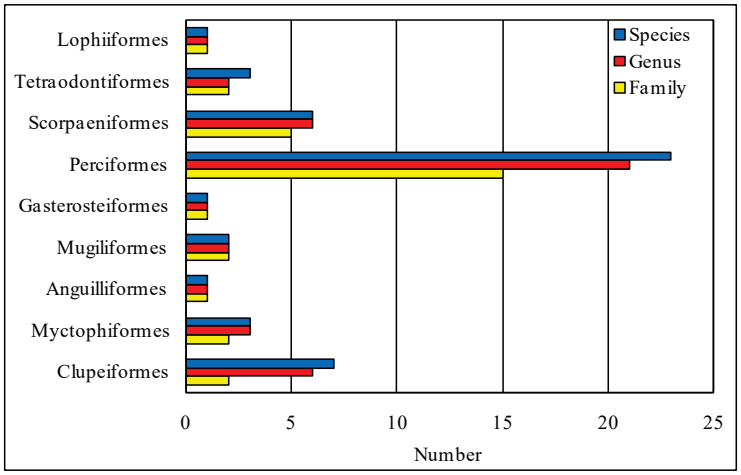

Figure R21-11. Fish catches composition in the Changjiang River estuary in 2004.

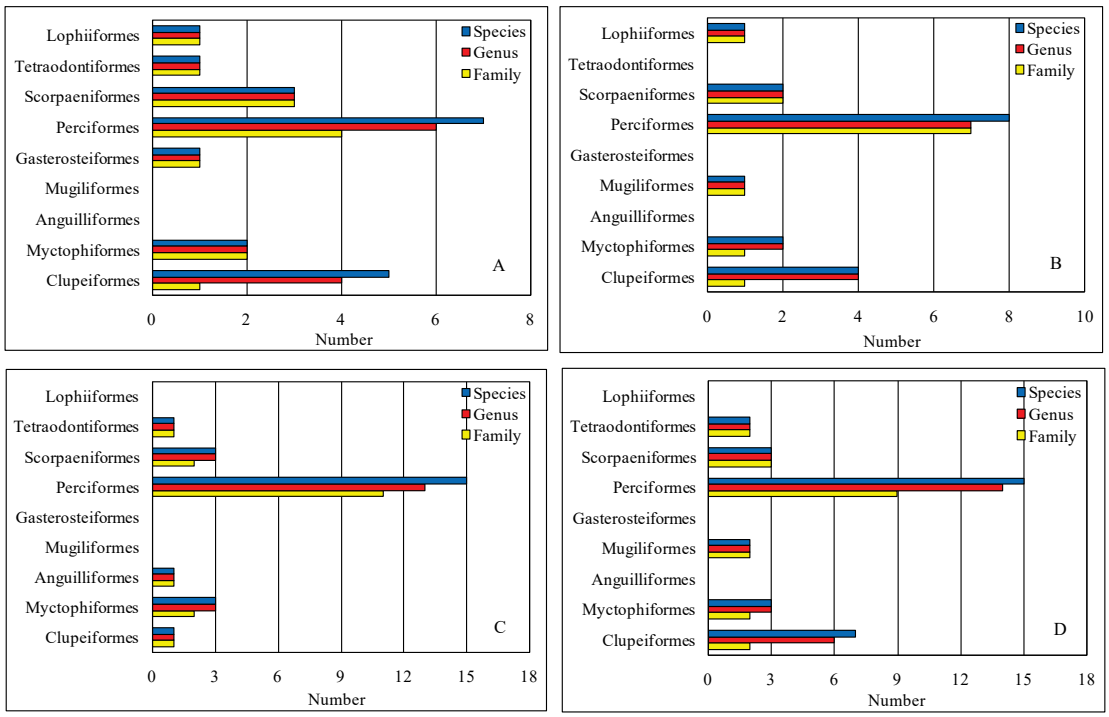

Figure R21-12. Fish community composition and monthly variation in the Changjiang River estuary and its adjacent area in 2004. A: spring, B: summer, C: autumn, D: winter.

Table R21-3. Fish species in the Changjiang River estuary in 2004.

Scientific name	February	May	August	November
Clupeiformes				
Clupeidae				
Ilisha elongata				+
Engraulidae				
Engraulis japonicus	+	+	+	+
Thrissa kammalensis	+			+
Coilia ectenes	+			+
Coilia mystus	+	+		+
Setipinna taty	+	+		+
Anchoviella commersonii		+		+
Myctophiformes				
Synpdidae				
Saurida elongata		+	+	+
Harpadon nehereus	+	+	+	+
Myctophidae				
Benthosema pterotum	+		+	+
Anguilliformes				
Muraenesocidae				
Muraenesox cinereus			+	
Scorpaeniformes				
Triglidae				
Lepidotrigla punctipectoralis		+	+	+
Aploactidae				
Erisphex potti	+	+		
Synanceiidae				
Minous monodactylus			+	
Vespicula sinensis			+	+
Platycephlidae				
Platycephalus indicus	+			+
Liparidae				
Liparis tanakae	+			

Table R21-3. Continued.

Scientific name	February	May	August	November
Tetraodontiformes				
Aluteridae				
Navodon septentrionalis				+
Tetraodontidae				
Fugu obscurus			+	+
Fugu alboplumbeus	+			
Lophiiformes				
Lophiidae				
Lophius litulon	+	+		

+ indicates occurrence.

8.1. Invertebrate community

In 2004, 27 species were sampled in the offshore area of the Changjiang River estuary, representing 19 Crustacea, 6 Mollusca and 2 Coelenterata. Crustacea was the predominant category in all four months, and no Coelenterates were observed during the survey conducted in February (Figure R21-13). All invertebrate species and their occurrence in different months are listed in Table R21-4.

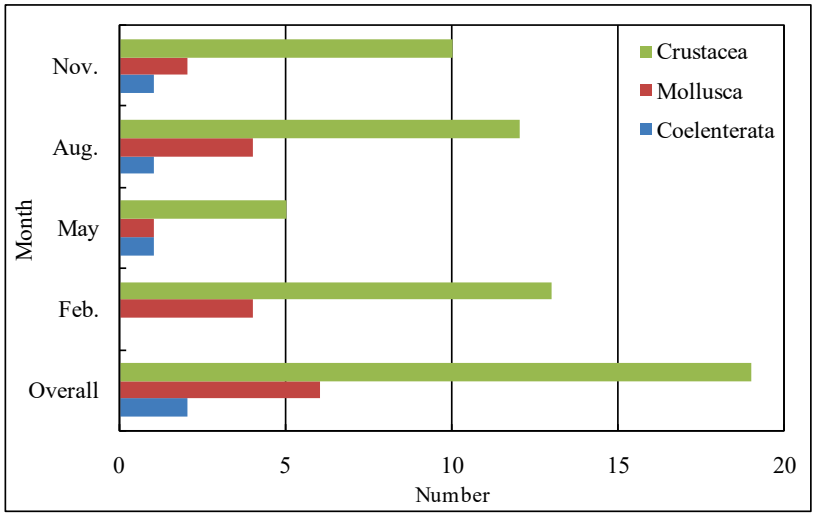

Figure R21-13. Invertebrate catches composition and monthly variation in the Changjiang River estuary and its adjacent area in 2004.

Table R21-4. Invertebrate species in the Changjiang River estuary in 2004.

Scientific name	February	May	August	November
Crustacea				
Oratosquilla oratoria	+	+	+	+
Charybdis bimaculata	+		+	+
Charybdis japonica	+		+	+
Portunus sanguinolentus	+		+	+
Portunus trituberculatus	+	+	+	+
Matuta planipes			+	
Neodorippe japonicum			+	
Calappidae		+		
Eucrate crenata				+
Crangon affinis	+			
Palaemon gravieri	+	+	+	+
Exopalaemon carinicauda	+			
Alpheus distinguendus	+			
Acetes chinensis	+			+
Penaeus spp.			+	
Penaeus orientalis			+	
Metapenaeopsis dalei	+		+	+
Trachypenaeus curvirostris	+	+	+	+
Leptochela gracilis	+			
Mollusca				
Loligo japonica	+	+	+	+
Euprymna spp.	+			
Sepiola birostrata	+			
Sepiola spp.	+		+	+
Octopus variabilis			+	
Hyriopsis cumingii			+	
Coelenterata				
Sanderia malayensis		+		
Rhopilema esculenta			+	+

9. References

Beardsley, R., Limeburner, R., Yu, H. and Cannon, G. 1985. Discharge of the Changjiang (Yangtze river) into the East China sea. Cont. Shelf Res. 4: 57–76, doi:10.1016/0278-4343(85)90022-6.

Chang, P.H. and Isobe, A. 2003. A numerical study on the Changjiang diluted water in the Yellow and East China Seas. J. Geophys. Res. Oceans 108: 3299, doi:10.1029/2002JC001749.

Chen, C.-C., Gong, G.-C. and Shiah, F.-K. 2007. Hypoxia in the East China Sea: One of the largest coastal low-oxygen areas in the world. Mar. Environ. Res. 64: 399–408, doi:10.1016/j.marenvres.2007.01.007.

Chen, C.-L., Zho, J.-C., Chen, M.-X., Gao, Z.-G. and Shum, C.-K. 2014. Sea level change under IPCC-A2 scenario in Bohai, Yellow, and East China Seas., Water Sci. Eng. 7: 446–456.

Chen, C.-T. A. 1996. The Kuroshio Intermediate Water is the major source of nutrients on the East China Sea continental shelf. Oceanol. Acta 19: 523–527.

Chen, C.-T.A. 2008. Distribution of nutrients in the East China Sea and the South China Sea connection. J. Oceanogr. 64: 737–751, doi:10.1007/s10872-008-0062-9.

Chen, C.-T.A. and Wang, S.-L. 1999. Carbon, alkalinity and nutrient budgets on the East China Sea continental shelf. J. Geophys. Res. Oceans 104: 20,675–20,686, doi:10.1029/1999JC900055.

Chen, C.-T.A., Ruo, R., Pai, S.C., Liu, C.T. and Wong, G.T.F. 1995. Exchange of water masses between the East China Sea and the Kuroshio off northeastern Taiwan. Cont. Shelf Res. 15: 19–39, doi: 10.1016/0278-4343(93)E0001-O.

Chen, D., Dai, Z., Xu, R., Li, D. and Mei, X. 2015. Impacts of anthropogenic activities on the Changjiang (Yangtze) estuarine ecosystem (1998–2012). Acta Oceanol. Sin. 34: 86–93, doi:10.1007/s13131-015-0679-7.

Chen, Y.L.L., Chen, H.-Y., Lee, W.-H., Hung, C.-C., Wong, G.T.F. and Kanda, J. 2001. New production in the East China Sea, comparison between well-mixed winter and stratified summer conditions. Cont. Shelf Res. 21: 751–764, doi:10.1016/S0278-4343(00)00108-4.

Dyhrman, S.T. and Ruttenberg, K.C. 2006. Presence and regulation of alkaline phosphatase activity in eukaryotic phytoplankton from the coastal ocean: Implications for dissolved organic phosphorus remineralization. Limnol. Oceanogr. 51: 1381–1390, doi:10.4319/lo.2006.51.3.1381.

Fang, G., Zhao, B. and Zhu, Y. 1991. Water volume transport through the Taiwan Strait and the continental shelf of the East China Sea measured with current meters. Elsevier Oceanogr. Ser. 54: 345–358, doi:10.1016/S0422-9894(08)70107-7.

Fang, T.-H. 2004. Phosphorus speciation and budget of the East China Sea. Cont. Shelf Res. 24: 1285–1299, doi:10.1016/j.csr.2004.04.003.

Gao, L., Li, D., Ishizaka, J., Zhang, Y., Zong, H. and Guo, L. 2015. Nutrient dynamics across the river-sea interface in the Changjiang (Yangtze River) estuary–East China Sea region. Limnol. Oceanogr. 60: 2207–2221, doi:10.1002/lno.10196.

Garrett, C. and Munk, W. 1975. Space-time scales of internal waves: A progress report. J. Geophys. Res. 80: 291–297, doi:10.1029/JC080i003p00291.

Gong, G.C. 2004. Absorption coefficients of colored dissolved organic matter in the surface waters of the East China Sea. Terr. Atmos. Ocean. Sci. 15: 75–87, doi:10.3319/TAO.2004.15.1.75(O).

Gong G.C., Chen, Y.L. and Liu, K.K. 1996. Chemical hydrography and chlorophyll a distribution in the East China Sea in summer: Implications in nutrient dynamics. Cont. Shelf Res. 16: 1561–1590.

Gong, G.-C., Chang, J., Chiang, K.-P., Hsiung, T.-M., Hung, C.-C., Duan, S.-W. and Codispoti, L.A. 2006. Reduction of primary production and changing of nutrient ratio in the East China Sea: Effect of the Three Gorges Dam? Geophys. Res. Lett. 33: L07610, doi:10.1029/2006GL025800.

Gordon, D.C., Boudreau, P.R., Mann, K.H., Ong, J.-E., Silvert, W.L., Smith, S.V., Wattayakorn, G., Wulff, F. and Yanagi, T. 1996. LOICZ Biogeochemical Modelling Guidelines. LOICZ Reports and Studies 5, LOICZ, Texel, The Netherlands, 96 pp.

Guan, B. and Chen, S. 1964. The current systems in the near-sea area of China Seas. Initial Rep. 5: 1–85.

Guan, B. and Fang, G. 2006. Winter counter-wind currents off the southeastern China coast: A review. J. Oceanogr. 62: 1–24, doi:10.1007/s10872-006-0028-8.

Guan, B.X. and Mao, H.L. 1982. A note on circulation of the East China Sea. Chin. J. Oceanol. Limnol. 1: 5–16.

Guo, X., Hukuda, H., Miyazawa, Y. and Yamagata, T. 2003. A triply nested ocean model for simulating the Kuroshio-Roles of horizontal resolution on JEBAR. J. Phys. Oceanogr. 33: 146–169, doi:10.1175/1520-0485(2003)033<0146:ATNOMF>2.0.CO;2.

Guo, X., Miyazawa, Y. and Yamagata, T. 2006. The Kuroshio onshore intrusion along the shelf break of the East China Sea: the origin of the Tsushima Warm Current. J. Phys. Oceanogr. 36: 2205–2231, doi:10.1175/jpo2976.1.

Guo, X., Zhu, X.-H., Wu, Q.-S. and Huang, D. 2012. The Kuroshio nutrient stream and its temporal variation in the East China Sea. J. Geophys. Res. Atmos. 117: C01026, doi:10.1029/2011JC007292.

Hu, J.Y. and Liu, M.S. 1992. The current structure during summer in southern Taiwan Strait. Trop. Oceanol. 11: 42–47 (in Chinese with English abstract).

Hung, C.-C., Gong, G.-C., Chou, W.-C., Chung, C.-C., Lee, M.-A., Chang, Y., Chen, H.-Y., Huang, S.-J., Yang, Y., Yang, W.-R., Chung, W.-C., Li, S.-L. and Laws, E. 2010. The effect of typhoon on particulate organic carbon flux in the southern East China Sea. Biogeosciences 7: 3007–3018, doi: 10.5194/bg-7-3007-2010.

Hung, C.-C., Chung, C.-C., Gong, G.-C., Jan, S., Tsai, Y., Chen, K.-S., Chou, W.C., Lee, M.-A., Chang, Y., Chen, M.-H., Yang, W.-R., Tseng, C.-J. and Gawarkiewicz, G. 2013. Nutrient supply in the Southern East China Sea after Typhoon Morakot. J. Mar. Res. 71: 133–149, doi:10.1357/002224013807343425.

Ichikawa, H. and Beardsley, R.C. 2002. The current system in the Yellow and East China Seas, J. Oceanogr. 58: 77–92, doi:10.1023/A:1015876701363.

Isobe, A., Ando, M., Watanabe, T., Senjyu, T., Sugihara, S. and Manda, A. 2002. Freshwater and temperature transports through the Tsushima-Korea Straits. J. Geophys. Res. Oceans 107: 3065, doi:10.1029/2000JC000702.

Jiang, Z., Liu, J., Chen, J., Chen, Q., Yan, X., Xuan, J. and Zeng, J. 2014. Responses of summer phytoplankton community to drastic environmental changes in the Changjiang (Yangtze River) estuary during the past 50 years. Water Res. 54: 1–11, doi:10.1016/j.watres.2014.01.032.

Kim, T.-W., Lee, K., Najjar, R.G., Jeong, H.-D. and Jeong, H.J. 2011. Increasing N abundance in the northwestern Pacific Ocean due to atmospheric nitrogen. Science 334: 505–509, doi:10.1126/science.1206583.

Kiyomoto, Y., Iseki, K. and Okamura, K. 2001. Ocean color satellite imagery and shipboard measurements of chlorophyll a and suspended particulate matter distribution in the East China Sea. J. Oceanogr. 57: 37–45, doi:10.1023/A:1011170619482.

Kondo, M. 1985. Oceanographic investigations of fishing grounds in the East China Sea and the Yellow Sea, 1: Characteristics of the mean temperature and salinity distributions measured at 50m and near the bottom. Bull. Seikai Region. Fish. Res. Lab. 62: 19–66

Le, K.-T. 1984. A preliminary study of the path of the Changjiang diluted water, Model. Oceanol. Limnol. Sin. 15: 157–167 (in Chinese with English abstract).

Li, D.J., Zhang, J., Huang, D.J., Wu, Y. and Liang, J. 2002. Oxygen depletion off the Changjiang (Yangtze River) Estuary. Sci. China Series D: Earth Sci. 45: 1137–1146.

Li, G., Han, X., Yue, S., Wen, G., Rongmin, Y. and Kusky, T. 2006. Monthly variations of water masses in the East China Seas. Cont. Shelf Res. 26: 1954–1970, doi:10.1016/j.csr.2006.06.008.

Li, H., Zhao, Y., Chen, X., Zhang, W., Xua, J., Li, J. and Xiao, T. 2016. Interaction between neritic and warm water tintinnids in surface waters of East China Sea. Deep Sea Res. II 124: 84–92, doi: 10.1016/j.dsr2.2015.06.008.

Li, J., Glibert, P.M., Zhou, M., Lu, S. and Lu, D. 2009. Relationships between nitrogen and phosphorus forms and ratios and the development of dinoflagellate blooms in the East China Sea. Mar. Ecol. Prog. Ser. 383: 11–26, doi:10.3354/meps07975.

Li, M., Xu, K., Watanabe, M. and Chen, Z. 2007. Long-term variations in dissolved silicate, nitrogen, and phosphorus flux from the Yangtze River into the East China Sea and impacts on estuarine ecosystem. Estuar. Coast. Shelf Sci. 71: 3–12, doi:10.1016/j.ecss.2006.08.013.

Li, R.G. 2003. Macrobenthos on the Continental Shelves and Adjacent Waters, China Sea. Ocean Press, Beijing.

Li X.Z. 2011. An overview of studies on marine macrobenthic biodiversity from Chinese waters: principally from the Yellow Sea. Biodiv. Sci. 19: 676–684, doi:10.3724/SP.J.1003.2011.09126.

Lian, E., Yang, S., Wu, H., Yang, C., Li, C. and Liu, J.T. 2016. Kuroshio subsurface water feeds the wintertime Taiwan Warm Current on the inner East China Sea shelf. J. Geophys. Res. Oceans 121: 4790–4803, doi:10.1002/2016JC011869

Lie, H.J. and Cho, C.H. 1994. On the origin of the Tsushima Warm Current. J. Geophys. Res. Oceans 99: 25,081–25,091, doi:10.1029/94JC02425.

Lim, H.-S., Diaz, R.J., Hong, J.-S. and Schaffner, L.C. 2006. Hypoxia and benthic community recovery in Korean coastal waters. Mar. Pollut. Bull. 52: 1517–1526, doi:10.1016/j.marpolbul.2006.05.013.

Limeburner, R., Beardsley, R.C. and Zhao, J. 1983. Water masses and circulation in the East China Sea. Proceedings of the International Symposium on Sedimentation on the Continental Shelf, with Special Reference to the East China Sea. China Ocean Press, Hangzhou, pp. 285–294.

Liu, H., Gong, G. and Chang, J. 2010. Lateral water exchange between shelf-margin upwelling and Kuroshio waters influences phosphorus stress in microphytoplankton. Mar. Ecol. Prog. Ser. 409: 121–130, doi:10.3354/meps08603.

Liu, K.-K., Tang, T.Y., Gong, G.-C., Chen, L.-Y. and Shiah, F.-K. 2000. Cross-shelf and along-shelf nutrient fluxes derived from flow fields and chemical hydrography observed in the southern East China Sea off northern Taiwan. Cont. Shelf Res. 20: 493–523, doi:10.1016/S0278-4343(99)00083-7.

Liu, K.-K., Yan, W., Lee, H.-J., Chao, S.-Y., Gong, G.-C. and Yeh, T.-Y. 2015. Impacts of increasing dissolved inorganic nitrogen discharged from Changjiang on primary production and seafloor oxygen demand in the East China Sea from 1970 to 2002. J. Mar. Syst. 141: 200–217, doi:10.1016/j.jmarsys.2014.07.022.

Liu, S.M., Zhang, J., Chen, H.T., Wu, Y., Xiong, H. and Zhang, Z.F. 2003. Nutrients in the Changjiang and its tributaries. Biogeochemistry 62: 1–18, doi:10.1023/A:1021162214304.

Liu, S.M., Hong, G.-H., Zhang, J., Ye, X.W. and Jiang, X.L. 2009. Nutrient budgets for large Chinese estuaries. Biogeosciences 6: 2245–2263, doi:10.5194/bg-6-2245-2009.

Liu, S.M., Qi, X.H., Li, X., Ye, H.R., Wu, Y., Ren, J.L., Zhang, J. and Xu, W.Y. 2016. Nutrient dynamics from the Changjiang (Yangtze River) estuary to the East China Sea. J. Mar. Syst. 154: 15–27, doi: 10.1016/j.jmarsys.2015.05.010.

Liu, X, Chiang, K.-P., Liu, S.-M., Wei, H., Zhao, Y. and Huang, B.-Q. 2015. Influence of the Yellow Sea Warm Current on phytoplankton community in the central Yellow Sea. Deep Sea Res. 106: 17–29, doi:10.1016/j.dsr.2015.09.008.

Liu, X., Xiao, W.P., Landry, M.R., Chiang, K.P., Wang, L. and Huang, B.Q. 2016. Responses of phytoplankton communities to environmental variability in the East China Sea. Ecosystems 19: 832–849, doi:10.1007/s10021-016-9970-5.

Liu, Z. and Hu, D. 2009. Preliminary study on the Huanghai Sea coastal current and its relationship with local wind in summer. Acta Oceanol. Sin. 31: 1–7 (in Chinese with English abstract).

Liu, Z., Wei, H., Lozovatsky, I. and Fernando, H. 2009. Late summer stratification, internal waves, and turbulence in the Yellow Sea. J. Mar. Syst. 77: 459–472, doi:10.1016/j.jmarsys.2008.11.001.

Lozovatsky, I., Jinadasa, P., Lee, J.H. and Fernando, H.J. 2015. Internal waves in a summer pycnocline of the East China Sea. Ocean Dyn. 65: 1051–1061, doi:10.1007/s10236-015-0858-2.

Mackin, J.E. and Aller, R.C. 1984. Ammonium adsorption in marine sediments. Limnol. Oceanogr. 29: 250–257.

Mackinnon J. and Gregg, M.C. 2005. Near-inertial waves on the New England Shelf: The role of evolving stratification, turbulent dissipation, and bottom drag. J. Phys. Oceanogr. 35: 2408–2424, doi:10.1175/JPO2822.1..

Mao, H., Gan, Z. and Lan, S. 1963. Preliminary study on the Changjiang diluted water and its mixing natures. Oceanol. Limnol. Sin. 5: 183–206 (in Chinese with English abstract).

Matsuno, T., Lee, J.-S., Shimizu, M., Kim, S.-H., Pang, I.-C. 2006. Measurements of the turbulent energy dissipation rate and an evaluation of th process of the Changjiang Diluted Water in the East China Sea. J. Geophys. Res. Oceans 111: C11S09, doi:10.1029/2005JC003196.

Miao, Y. and Yu, H. 1991. Spatial and temporal variations of water type mixing characteristic in the East China Sea. Trans. Sci. Survey Kuroshio Current 3: 193–203.

Minakawa, M. and Watanabe, Y. 1998. Aluminum in the East China Sea and Okinawa Trough, marginal sea areas of the western North Pacific. J. Oceanogr. 54: 629–640, doi:10.1007/BF02823283.

Moon, J.H., Hirose, N., Yoon, J.H. and Pang, I.C. 2010. Offshore detachment process of the low-salinity water around Changjiang Bank in the East China Sea. J. Phys. Oceanogr. 40: 1035–1053, doi:10.1175/2010jpo4167.1.

Mulholland, M.R., Floge, S., Carpenter, E.J. and Capone, D.G. 2002. Phosphorus dynamics in cultures and natural populations of *Trichodesmium* spp. Mar. Ecol. Prog. Ser. 239: 45–55, doi:10.3354/meps239045.

Ning, X., Liu, Z., Cai, Y. and Fang, M. 1998. Physicobiological oceanographic remote sensing of the East China Sea: Satellite and in situ observations. J. Geophys. Res. Oceans 103: 21,623–21,635, doi:10.1029/98JC01612.

Nitani, H. 1972. Beginning of the Kuroshio, pp. 129-163 in: Kuroshio—Its Physical Aspects edited by H. Stommel and K. Yoshida Kuroshio, University of Tokyo Press, Tokyo.

Office of Integrated Oceanographic Survey of China. 1961. Dataset of the national integrated oceanographic survey. vol 1. Survey data of hydrometeorological and chemical elements in the bohai, Huanghai and East China Seas, Beijing, 811 pp.

Qi, J., Yin, B., Zhang, Q., Yang, D. and Xu, Z. 2014. Analysis of seasonal variation of water masses in East China Sea. Chin. J. Oceanol. Limnol. 32: 958–971, doi:10.1007/s00343-014-3269-1.

Qiu, B. and Imasato, N. 1990. A numerical study on the formation of the Kuroshio Counter Current and the Kuroshio Branch Current in the East China Sea. Cont. Shelf Res. 10: 165–184, doi:10.1016/0278-4343(90)90028-k.

Ren, J, Zhang, J. and Liu, S. 2005. A review on aluminum to titanium ratio as a geochemical proxy to reconstruct paleoproductivity. Advances Earth Sci. 20: 1314.

Ren, J.L., Zhang, J., Li, J.B., Yu, X.Y., Liu, S.M. and Zhang, E.R. 2006. Dissolved aluminum in the Yellow Sea and East China Sea – Al as a tracer of Changjiang (Yangtze River) discharge and Kuroshio incursion. Estuar. Coast. Shelf Sci. 68: 165–174, doi:10.1016/j.ecss.2006.02.004.

Ren, J.L., Xuan, J.L., Wang, Z.W., Huang, D. and Zhang, J. 2015. Cross-shelf transport of terrestrial Al enhanced by the transition of northeasterly to southwesterly monsoon wind over the East China Sea. J. Geophys. Res. Oceans 120: 5054–5073, doi:10.1002/2014JC010655.

Shi, W. and Wang, M. 2009. An assessment of the black ocean pixel assumption for MODIS SWIR bands. Remote Sens. Environ. 113: 1587–1597.

Shiozaki, T., Furuya, K., Kodama, T., Kitajima, S., Takeda, S., Takemura, T. and Kanda, J. 2010. New estimation of N fixation in the western and central Pacific Ocean and its marginal seas. Global Biogeochem. Cycles 24: GB1015, doi:10.1029/2009GB003620.

Siswanto, E., Nakata, H., Matsuoka, Y., Tanaka, K., Kiyomoto, Y., Okamura, K., Zhu, J. and Ishizaka, J. 2008a. The long-term freshening and nutrient increases in summer surface water in the northern East China Sea in relation to Changjiang discharge variation. J. Geophys. Res. Atmos. 113: C10030, doi:10.1029/2008JC004812.

Siswanto, E., Ishizaka, J., Morimoto, A., Tanaka, K., Okamura K., Kristijono, A. and Saino, T. 2008b. Ocean physical and biogeochemical responses to the passage of Typhoon Meari in the East China Sea observed from Argo float and multiplatform satellites. Geophys. Res. Lett. 35: L15604, doi: 10.1029/2008GL035040.

Siswanto, E., Morimoto, A. and Kojima, S. 2009. Enhancement of phytoplankton primary productivity in the southern East China Sea following episodic typhoon passage. Geophys. Res. Lett. 36: L11603, doi:10.1029/2009GL037883.

Su, H., Yang, R.J., Zhang, A.B. and Li, Y. 2015. Dissolved iron distribution and organic complexation in the coastal waters of the East China Sea. Mar. Chem, 173: 208–221, doi:10.1016/j.marchem.2015.03.007.

Su, H., Yang, R., Zhang, A., Li, Y., Qu, S. and Wang, X. 2017. Characteristics of trace metals and phosphorus in seawaters offshore the Yangtze River. Mar. Pollut. Bull. 124: 1020–1032, doi: 10.1016/j.marpolbul.2017.01.022.

Su, J. and Pan, Y. 1987. On the shelf circulation north of Taiwan. Acta Oceanol. Sin. 6(Suppl. 1): 1–20.

Su, J. and Wang, W. 1987. On the sources of the Taiwan Warm Current from the South China Sea. Chin. J. Oceanol. Limnol. 5: 299–308, doi:10.1007/BF02843812.

Su, J., Pan, Y. and Liang, X. 1994. Kuroshio intrusion and Taiwan Warm Current, pp. 59–70 in: Oceanology of China Seas, vol. 1 edited by D. Zhou, Y.-B. Liang and C.-K. Zeng (C.K. Tseng), Kluwer Academic, Dordrecht.

Su, Y.S. and Weng, X.C. 1994. Water masses in China seas, pp. 3–16 in: Oceanology of China Seas, vol. 1 edited by D. Zhou, Y.-B. Liang and C.-K. Zeng (C.K. Tseng), Kluwer Academic, Dordrecht.

Sun, M.S., Zhang, G.L., Ma, X., Cao, X.P., Mao, X.Y., Li, J., Ye, W.W. and Liu, S.M. 2018. Dissolved methane in the East China Sea: Distribution, seasonal variation and emission. Mar. Chem. 202: 12–26, doi:10.1016/j.marchem.2018.03.001.

Sun S. 2012. Regional Oceanography of China Seas - Biological Oceanography. Ocean Press, Beijing.

Takikawa, T., Yoon, J.-H. and Cho, K.-D. 2005. The Tsushima Warm Current through Tsushima Straits estimated from ferryboat ADCP data. J. Phys. Oceanogr. 35: 1154–1168, doi:10.1175/JPO2742.1.

Tang, D.L., Ni, I.H., Muller-Karger, F.E. and Liu, Z.J. 1998. Analysis of annual and spatial patterns of CZCS-derived pigment concentration on the continental shelf of China. Cont. Shelf Res. 18: 1493–1515, doi:10.1016/S0278-4343(98)00039-9.

Tian, R.C., Hu, F.X. and Martin, J.M. 1993. Summer nutrient fronts in the Changjiang (Yantze River) Estuary. Estuar. Coast. Shelf Sci. 37: 27–41, doi:10.1006/ecss.1993.1039.

Tishchenko, P.Y., Lobanov, V.B., Zvalinsky, V.I., Sergeev, A.F., Koltunov, A., Mikhailik, T.A., Tishchenko, P.P., Shvetsova, M.G., Sagalaev, S. and Volkova, T. 2013. Seasonal hypoxia of Amursky Bay in the Japan Sea: Formation and destruction. Terrest. Atmos. Ocean. Sci. 24: 1033–1050, doi: 10.3319/tao.2013.07.12.01(oc).

Turner, R.E., Rabalais, N.N. and Justić, D. 2012. Predicting summer hypoxia in the northern Gulf of Mexico: Redux. Mar. Pollut. Bull. 64: 319–324, doi:10.1016/j.marpolbul.2011.11.008.

Wang, B.D. 2006. Cultural eutrophication in the Changjiang (Yangtze River) plume: History and perspective. Estuar. Coast. Shelf Sci. 69: 471–477, doi:10.1016/j.ecss.2006.05.010.

Wang, B.D. 2009. Hydromorphological mechanisms leading to hypoxia off the Changjiang estuary. Mar. Environ. Res. 67: 53–58, doi:10.1016/j.marenvres.2008.11.001.

Wang, B.D. and Wang, X.L. 2007. Chemical hydrography of coastal upwelling in the East China Sea. Chin. J. Oceanol. Limnol. 25: 16–26, doi:10.1007/s00343-007-0016-x

Wang, B-D., Wang, X-L. and Zhan, R. 2003. Nutrient conditions in the Yellow Sea and the East China Sea. Estuar. Coast. Shelf Sci. 58: 127–136, doi:10.1016/S0272-7714(03)00067-2.

Wang, B.D., Wei, Q.S., Chen, J.F. and Xie, L.P. 2012. Annual cycle of hypoxia off the Changjiang (Yangtze River) Estuary. Mar. Environ. Res. 77: 1–5, doi:10.1016/j.marenvres.2011.12.007.

Wang, Z., Ren, J., Jiang, S., Liu, S., Xuan, J. and Zhang, J. 2016. Geochemical behavior of dissolved manganese in the East China Sea: seasonal variation, estuarine removal, and regeneration under suboxic conditions. Geochem. Geophys. Geosyst. 17: 282–299, doi:10.1002/2015GC006128.

Weng, X. and Wang, C. 1984. A preliminary study on the TS characteristics and the origin of Taiwan Warm Current Water in summer. Stud. Mar. Sinica 21: 113–133 (in Chinese with English abstract).

Wu, C., Fu, F-X., Sun J., Thangaraj S. and Pujari L. 2018. Nitrogen fixation by *Trichodesmium* and unicellular diazotrophs in the northern South China Sea and the Kuroshio in summer. Sci. Rep. 8: 2415, doi:10.1038/s41598-018-20743-0.

Wu, H., Zhu, J., Shen, J. and Wang, H. 2011. Tidal modulation on the Changjiang River plume in summer. J. Geophys. Res. Oceans 116: C08017, doi:10.1029/2011JC007209.

Wu, Y., Zhang, J., Li, D.J., Wei, H. and Lu, R.X. 2003. Isotope variability of particulate organic matter at the PN section in the East China Sea. Biogeochemistry 65: 31–49, doi:10.1023/A:1026044324643.

Xu, Y.J., Ishizaka, J., Yamaguchi, H., Siswanto, E. and Wang, S.Q. 2013. Relationships of interannual variability in SST and phytoplankton blooms with giant jellyfish (*Nemopilema nomurai*) outbreaks in the Yellow Sea and East China Sea. J. Oceanogr. 69: 511–526, doi:10.1007/s10872-013-0189-1.

Yamaguchi, H., Kim, H.-C., Son, Y.B., Kim, S.W., Okamura, K., Kiyomoto, Y. and Ishizaka, J. 2012. Seasonal and summer interannual variations of SeaWiFS chlorophyll alpha in the Yellow Sea and East China Sea. Prog. Oceanogr. 105: 22–29, doi:10.1016/j.pocean.2012.04.004.

Yamaguchi, H., Ishizaka, J., Siswanto, E., Son, Y.B., Yoo, S. and Kiyomoto, Y. 2013. Seasonal and spring interannual variations in satellite-observed chlorophyll-a in the Yellow and East China Seas: New datasets with reduced interference from high concentration of resuspended sediment. Cont. Shelf Res. 59: 1–9, doi:10.1016/j.csr.2013.03.009.

Yang, D., Yin, B., Liu, Z. and Feng, X. 2011. Numerical study of the ocean circulation on the East China Sea shelf and a Kuroshio bottom branch northeast of Taiwan in summer. J. Geophys. Res. Oceans 116: C05015, doi:10.1029/2010JC006777.

Yang, D., Yin, B., Liu, Z., Bai, T., Qi, J. and Chen, H. 2012. Numerical study on the pattern and origins of Kuroshio branches in the bottom water of southern East China Sea in summer. J. Geophys. Res. Oceans 117: C02014, doi:10.1029/2011JC007528.

Yang, W., Wei, H. and Zhao, L. 2017. Observations of tidal straining within two different ocean environments in the East China Sea: Stratification and near-bottom turbulence. J. Geophys. Res. Oceans 122: 8876–8893, doi:10.1002/2017JC012924.

Yuan, D. and Hsueh, Y. 2010. Dynamics of the cross-shelf circulation in the Yellow and East China Seas in winter. Deep Sea Res. II: 57: 1745–1761, doi:10.1016/j.dsr2.2010.04.002.

Yuan, D., Zhu, J., Li, C. and Hu, D. 2008. Cross-shelf circulation in the Yellow and East China Seas indicated by MODIS satellite observations. J. Mar. Syst. 70: 134–149, doi:10.1016/j.jmarsys.2007.04.002.

Zhang, G., Zhang, J., Ren, J., Li, J. and Liu, S. 2008a. Distributions and sea-to-air fluxes of methane and nitrous oxide in the North East China Sea in summer. Mar. Chem. 110: 42–55, doi:10.1016/j.marchem.2008.02.005.

Zhang, G., Zhang, J., Liu, S., Ren, J., Xu, J. and Zhang, F. 2008b. Methane in the Changjiang (Yangtze River) Estuary and its adjacent marine area: Riverine input, sediment release and atmospheric fluxes. Biogeochemistry 91: 71–84, doi: 10.1007/s10533-008-9259-7.

Zhang, G.L., Zhang, J., Kang, Y.B. and Liu, S.M. 2004. Distributions and fluxes of methane in the East China Sea and the Yellow Sea in spring. J. Geophys. Res. Oceans 109: doi:10.1029/2004JC002268.

Zhang, G.T., Sun, S. and Zhang, F. 2005. Seasonal variation of reproduction rates and body size of *Calanus sinicus* in the Southern Yellow Sea, China. J. Plankt. Res. 27: 135–143, doi:10.1093/plankt/fbh164.

Zhang, J. and Su, J.L. 2006. Nutrient dynamics of the China Seas: the Bohai Sea, Yellow Sea, East China Sea and South China Sea, pp. 637–671 in: The Sea, vol. 14 edited by A.R. Robinson and K.H. Brink, Harvard University Press, Cambridge.

Zhang, J., Zhang, Z.F., Liu, S.M., Wu, Y., Xiong, H. and Chen, H.T. 1999. Human impacts on the large world rivers: Would the Changjiang (Yangtze River) be an illustration? Global Biogeochem. Cycles 13: 1099–1105, doi:10.1029/1999GB900044.

Zhang, J., Liu, S.M., Ren, J.L., Wu, Y. and Zhang, G.L. 2007. Nutrient gradients from the eutrophic Changjiang (Yangtze River) Estuary to the oligotrophic Kuroshio waters and re-evaluation of budgets for the East China Sea Shelf. Progr. Oceanogr. 74: 449–478, doi:10.1016/j.pocean.2007.04.019.

Zhang, J., Liu, Q., Bai, L-L. and Matsuno, T. 2018. Water mass analysis and contribution estimation using heavy rare earth elements: Significance of Kuroshio intermediate water to Central East China Sea shelf water. Mar. Chem. 204: 174–180, doi:10.1016/J.MARCHEM.2018.07.011.

Zhu, J. and Shen, H. 1997. Extension mechanisms of Changjiang Diluted Water. East China Normal University Press, Shanghai, pp. 18–176 (in Chinese with English abstract).

Zhu, J., Xiao, C. and Shen, H. 1998. Numerical model simulation of expansion of Changjiang diluted water in summer. Acta Oceanol. Sin. 20: 13–22 (in Chinese with English abstract).

Zhu, M.Y., Li, R.X., Mu, X.Y. and Ji, R.B. 1997. Harmful algal blooms in China seas. Ocean Res. 19: 173–184.

Zhu, Y., Ishizaka, J., Tripathy, S.C., Wang, S., Sukigara, C., Goes, J., Matsuno, T. and Suggett, D.J. 2017. Relationship between light, community composition and the electron requirement for carbon fixation in natural phytoplankton. Mar. Ecol. Prog.Ser. 580: 83–100, doi:10.3354/meps12310.

Zhu, Z.Y., Zhang, J., Wu, Y., Zhang, Y.Y., Lin, J. and Liu, S.M. 2011. Hypoxia off the Changjiang (Yangtze River) Estuary: Oxygen depletion and organic matter decomposition. Mar. Chem. 125: 108–116, doi:10.1016/j.marchem.2011.03.005.

Zhu, Z.Y., Wu, Y., Zhang, J., Du, J.Z. and Zhang, G.S. 2014. Reconstruction of anthropogenic eutrophication in the region off the Changjiang Estuary and central Yellow Sea: From decades to centuries. Cont. Shelf Res. 72: 152–162, doi:10.1016/j.csr.2013.10.018.

Zhu, Z.-Y., Hu, J., Song, G.-D., Wu, Y., Zhang, J. and Liu, S.M. 2016. Phytoplankton-driven dark plankton respiration in the hypoxic zone off the Changjiang Estuary, revealed by in vitro incubations. J. Mar. Syst. 154: 50–56, doi:10.1016/j.jmarsys.2015.04.009.

Zhu, Z.-Y., Wu, H., Liu, S.-M., Wu, Y., Huang, D.-J., Zhang, J. and Zhang, G.-S. 2017. Hypoxia off the Changjiang (Yangtze River) estuary and in the adjacent East China Sea: Quantitative approaches to estimating the tidal impact and nutrient regeneration. Mar. Pollut. Bull. 125: 103–114,doi:10.1016/j.marpolbul.2017.07.029.

Zilius, M., Bartoli, M., Bresciani, M., Katarzyte, M., Ruginis, T., Petkuviene, J., Lubiene, I., Giardino, C., Bukaveckas, P.A., de Wit, R. and Razinkovas-Baziukas, A. 2014. Feedback mechanisms between cyanobacterial blooms, transient hypoxia, and benthic phosphorus regeneration in shallow coastal environments. Estuar. Coasts 37: 680–694, doi:10.1007/s12237-013-9717-x.